# Final Report

## Development and Application of Methods for Modelling and Mapping Ozone Deposition and Stomatal Flux

EPG 1/3/173

October 2000 – September 2003

# EXECUTIVE SUMMARY


- Ozone impacts on vegetation depend to a large extent on the uptake of ozone through the stomata. Ozone deposition to land surfaces across Europe is a function of this stomatal uptake, together with non-stomatal deposition to the soil and to external plant surfaces.

- At the start of this project, in 2000, risk assessment within UN/ECE for ozone impacts on vegetation in Europe was based on cumulative exposure to external ozone concentrations, using the AOT40 index, rather than on modelled flux through the stomata. At the same time, the EMEP photo-oxidant model, which was used within UN/ECE to predict changes in ozone concentration fields across Europe in response to changing precursor emissions, used a simple surface resistance parameterisation to model deposition which did not include the effects of variable stomatal conductance.

- The major aim of this project was to further develop and evaluate models of ozone deposition and stomatal flux that had been developed in previous work. The ultimate objective of the work was to link these models to the EMEP photo-oxidant model and hence to model ozone deposition and stomatal flux to different land covers, and to individual species, across Europe.

- A substantial number of studies have been performed to evaluate the performance of both the deposition and stomatal flux models using field data. In general terms, the model performed well in most of these evaluations, and was able to predict the magnitude of, as well as the diurnal and seasonal variation in, measured ozone deposition velocities to a range of vegetation types. Less data is available for evaluation in Mediterranean regions, and those comparisons that have been made indicate that model performance could be improved. Access to micrometeorological data for Californian vineyards has allowed some important changes to be identified to the model parameterisation for this major Mediterranean crop.

- A number of changes in the model formulation have been made as a result of the evaluations against field data. The major changes include:- (i) incorporation of thermal time models for wheat and potato to predict variation in growing seasons across Europe; (ii) modelling of individual leaf populations in deterministic crops such as wheat; (iii) improved modelling of phenological variation in stomatal conductance in temperate tree species; (iv) changes in the functions describing stomatal responses to light to allow night-time opening to be modelled when required; and (v) revision of the functions describing stomatal responses to temperature, to allow asymmetrical variation around the optimal temperature.

- The parameterisation of the stomatal flux model has also been substantially revised through a process of literature review and continued dialogue with

scientists across Europe who are involved in both experimental studies and modelling. In particular, the parameterisation for both wheat and potato was substantially altered, as part of the process of developing flux-response relationships for these major crop species, and the parameterisation for trees underwent a major comprehensive revision. These changes in parameterisation, as with the revised formulations, have led to better agreement with observed variations in stomatal conductance.

- The SEI land cover map that is used in spatial modelling of ozone flux and deposition has been updated, following a comparison with the CORINE and PELCOM data sets. The major improvements include:- (i) an extension of the spatial coverage and incorporation of national boundaries; (ii) increased detail in classification of dominant forest species, grassland types and cropping patterns; (iii) incorporation of new data on crop distributions; and (iv) the inclusion of data on irrigation patterns. The updated SEI land cover map has now been made freely available to users to complement other national or European datasets.

- The sensitivity of estimates of national yield losses due to ozone to uncertainty in the land cover map was evaluated for wheat for the U.K.. Uncertainty in yield was lowest in grid squares with high or low coverage of wheat and greatest in those with moderate coverage. Yield losses were over-estimated when using the SEI land cover map compared with Defra statistics on wheat coverage.

- Laboratory and field studies were conducted to further test and develop a model of detoxification of ozone in the cell wall through reaction with ascorbate. Chemical treatments to enhance ascorbate activity and use of transgenic plants with high ascorbate oxidase activity provided further evidence that high levels of ascorbate activity reduce the impact of ozone, by detoxifying the incoming flux.

- Field measurements of wheat in both the UK and Spain showed a strong diel variation in ascorbate concentration in the cell wall, which suggests that detoxification of incoming flux is greatest in the middle of the day. These data were combined with data on stomatal conductance in the model to calculate the ozone flux to the plasmalemma, the primary site of damage in the leaf. These fluxes shown strong diel variations and were higher in the UK than in Spain, suggesting that the same ozone concentration would have a larger impact on wheat in the UK. The potential has been identified for approaches that link the stomatal flux and ozone detoxification models, and hence allow a more mechanistic approach to ozone risk assessment.

- The impact of increasing global background ozone concentrations in the UK was modelled, and assessed in the context of possible impacts on vegetation. In addition to increases in mean concentration, the length of time for which vegetation may be exposed to significant ozone concentrations, especially in early spring, will be increased. Since ozone flux models show that significant ozone fluxes may occur in sensitive species with external concentrations in the range 20-40ppb, it should not be assumed that gradual increases in background

concentrations within this range are not of biological consequences. Hence, the use of flux based approaches rather than the AOT40 index will provide a stronger basis to assess the significance of increased global background ozone concentrations.

- The work under this contract has had a significant influence within the policy framework of UN/ECE over the past three years. The Gothenburg workshop, in November 2002, recommended that flux-based critical levels should be established for ozone. Subsequently, detailed methods to derive such critical levels, and map their exceedances, have been agreed, and have been formally incorporated in the Mapping Manual, for wheat, potato and for sensitive trees species such as beech. Modified versions of our flux models, developed by collaboration between Swedish research groups, were used as the basis for these new critical levels. In addition, a new flux and deposition algorithm has now been incorporated into the new Unified EMEP Model, which for ozone is based on the work under this, and previous, contracts. A recent evaluation workshop concluded that the new EMEP model was suitable as the basis of future risk assessment methods for ozone at a European scale.

- The development of a consistent approach to the use of flux models in both formulating critical levels, and in modelling continental-scale ozone deposition and flux, ensures that there is now a consistent methodological approach on which flux-based methods can be used to evaluate the impacts of ozone on vegetation under different policy scenarios. This is a major development in ozone risk assessment to which the work under this contract has made a significant contribution. However, further work is needed to evaluate and improve model formulation and parameterisation and to develop flux-based critical levels for a wider range of vegetation.

# Contents

# 1 Introduction and overview

Ozone impacts on vegetation depend to a large extent on the uptake of the pollutant through the stomata. Ozone deposition to land surfaces across Europe is a function of this stomatal uptake, together with non-stomatal deposition to the soil and to external plant surfaces. Stomatal conductance, and hence ozone flux, is sensitive to a number of environmental factors, such as irradiance, temperature, vapour pressure deficit and soil moisture deficit, as well as vegetation phenology. The nature of these responses means that days of high ozone concentration, and regions across Europe experiencing high ozone episodes, are not necessarily those associated with the highest ozone flux and deposition. This means that the greatest impacts of ozone on vegetation will not necessarily be associated with those areas experiencing the highest ozone exposures, a fact which has considerable significance in assessing the cost-effectiveness of regional measures to reduce precursor emissions.

At the time that this project began in 2000, the AOT40 index, based on cumulative exposure to external ozone concentrations, was used to assess the potential impact of ozone on vegetation at a European scale. Although it had been accepted at the UN/ECE Gerzensee workshop, held in April 1999, that ozone flux provided a stronger basis than AOT40 for quantifying the impacts of ozone, no suitable models of ozone flux were available for detailed evaluation and application. At the same time, the EMEP photo-oxidant model, used to predict ozone concentration fields across Europe, and their response to changing emission rates of ozone precursors, used a relatively crude surface resistance parameterisation which did not incorporate the effects of environmental variables on stomatal conductance and total ozone deposition, and hence on the modelled mass balance of ozone across the continent.

The major aim of this project was to further develop and evaluate models of ozone deposition and stomatal flux, linking them with the EMEP photo-oxidant model to predict ozone deposition and stomatal flux of ozone to different land covers, and to specific species, across Europe. In broad terms, the project has been highly successful and has had a significant influence within the policy framework of UN/ECE. This was reflected in the positive outcome of the Gothenburg workshop on Level II critical levels of ozone, which was held in November 2002 (Karlsson et al. 2003). General conclusions from this workshop were that substantial progress had been made in the development of new ozone critical levels for agricultural crops, semi-natural vegetation and forests, including those based on flux. The work in this contract has been instrumental in forming the basis on which the flux based approach has been used to derive critical fluxes of ozone for two agricultural crops, wheat and potato, across Europe, and provisionally for sensitive forest trees, such as beech, which have now been formally adopted within the UN/ECE Mapping Manual. At the same time, our work with EMEP has resulted in the incorporation of similar flux and deposition algorithms within the deposition module of the new Unified EMEP model (Simpson et al., 2003). A recent evaluation workshop judged that the new EMEP model was suitable for forming the

basis of future ozone risk assessment methods at the European scale. The development of a consistent approach to the use of flux models in both formulating critical levels, and modelling continental-scale deposition and flux, ensures that there is a consistent methodological approach on which on which flux-based methods can be used to evaluate the impacts of ozone on vegetation under different policy scenarios. This is a major development in ozone risk assessment to which the work under this contract has made a significant contribution. It is very important to recognise that we are only one of a number of research groups who have contributed to these major developments in ozone risk assessment tools, and that such rapid progress has only been possible through very active and positive collaboration between the different research groups.

This final report provides a brief summary of the progress made in each section of the work-programme, with some more detail of work carried out over the last six months. The programme has generated a substantial number of written and electronic outputs, and reference and links to these are provided for more detail on the work that has been undertaken. Some changes have been made to the original work programme, in consultation with the DEFRA project officer, primarily to ensure that our work made the most effective contribution to the development of flux-based risk assessment methods for ozone, and, most importantly, their acceptance for application within the UN/ECE framework. This final report is therefore structured in terms of the major areas of actual work and key outcomes, rather than the original work packages. These are as follows:-

- Evaluation of stomatal flux and deposition models
- Improvements to the parameterisation and formulation of the flux model
- Development of land-cover database
- Modelling of ozone detoxification
- Impacts of increased global background ozone levels
- Policy outcomes within ICP Vegetation and EMEP
- Dissemination

# 2 Evaluation of stomatal flux and deposition models

## 2.1 Summary of Project work.

Over the past three years, a substantial number of studies have been performed to evaluate both the deposition and stomatal flux models. These evaluations have been performed either directly by members of the project consortium or by colleagues in Europe who have been in close contact with the project collaborators to ensure that evaluations are performed using appropriate model formulation and parameterisation.

Details of each of these evaluations have been recorded either in previous Defra reports (where the evaluations were made by project members) or in the peer reviewed literature (as cited in the dissemination section of the relevant Defra report). As such, only short summaries of these studies are provided within this section. To clearly indicate the progress that has been made to date with this evaluation work it is also useful to summarise all the studies that have been performed (in relation to the cover types and species investigated) and indicate the predictive capabilities of the model for each evaluation. Table 2.1 provides such a summary.

Table 2.1 shows that, on the whole, the model has performed well in many of the evaluation studies performed. The model performance in these cases is assessed according to the capabilities of the model to describe the magnitude, as well as diurnal and seasonal variations, of deposition velocities. In most cases, model performance can be improved by parameterising the model according to local data; however, this is to be expected given that the model is designed for application at the regional scale and the evaluations are performed on a site-specific basis.

The Table also shows that there are some cover types for which the model performance still needs to be evaluated. These are mostly those cover types associated with Mediterranean regions; where evaluations of such Mediterranean vegetation have been made, the model performs less well which reflects the reduced availability of data to parameterise for these regions. Efforts are underway to resolve these data issues through closer collaboration with colleagues in Spain and Italy.

The following sections summarise the key evaluation studies made by CEH Edinburgh as part of this project, and the describes in more detail a recently completed comparison to investigate the model's predictive abilities against field data for vineyards collected in California.

Table 2.1. Summary of studies performed to evaluate either total ozone deposition or stomatal / surface ozone deposition.

| Deposition class | Species | Location | Total deposition | Stomatal / surface deposition | Reference |
|---|---|---|---|---|---|
| Temperate coniferous | Scots Pine | Finland | Good | Good | Altimir et al. (sub) |
| | Norway spruce | Denmark | | Average | Tuovinen et al. (2001b) |
| | Norway spruce | Austria | | Good | Emberson et al. (2000) |
| Temperate boreal | Birch | Finland | Average | Average | Tuovinen et al. (2001b) |
| | Beech | Germany | | Good | Baumgarten et al. (2000) |
| Mediterranean Needle leaf | | | | | |
| Mediterranean broadleaf | Kermes oak | Spain | | Poor | Nali et al (sub) |
| Temperate crops | Wheat | Italy | Good | Good | Tuovinen et al. (sub) |
| | Sugar beet, Oats & wheat | Scotland | Average | Average | Defra report |
| Mediterranean crops | | | | | |
| Root crops | | | | | |
| Vineyards | Grapevine | California, USA | Good | Average | This report |
| Temperate orchard | | | | | |
| Mediterranean orchard | | | | | |
| Grassland | *Festuca, Trifolium* spp. | Portugal | | Poor | Tuovinen et al. (2001b) |
| | Lolium | Scotland | | Good | Coyle et al. (sub) |
| Semi-natural | *Deschampsia, Molina, Carex, Eriphorum* spp. | Scotland | Good | | Defra report |
| Mediterranean scrub | | | | | |
| Wetlands | sub-arctic fen | Finland | Average | Good | Tuovinen et al. (2001b) |
| Tundra | | | | | |

## 2.2 CEH Deposition data

This work compared observed and modelled predictions of ozone flux to two different land-cover types i) agricultural crops (including sugar beet, oats and wheat) and ii) semi-natural grasslands (dominated by *Lolium perenne*). The measurements made for the agricultural land-cover type (located at Sutton Bonnington, near Nottingham, U.K.) used aerodynamic flux gradient methods to calculate total ozone deposition. Deposition measurements to the grassland cover-type (located at Easter Bush, near Edinburgh, U.K.) were made using both eddy-correlation and aerodynamic flux gradient methods. Additional energy-balance measurements made at this site enabled the quantification of canopy resistance for water vapour exchange and hence allowed differentiation between stomatal and non-stomatal components of ozone deposition.

Results showed that at both sites the model was capable of reproducing the basic meteorological resistances and variables satisfactorily. In terms of total ozone deposition estimates, the model performance varied at each site and for the different crop types at the Sutton Bonnington location, although periods were found for each of the data sets where the measurements and model predictions were in close agreement. The model seemed to perform best for oats at the Sutton Bonnington site. For example, Figure 2.2 shows diurnal cycles of hourly measured and modelled ozone deposition velocities over sugar beet and oats from which it is evident that close agreement exists between modelled and measured values. However, these data also suggest that large and small values of deposition velocity tend to be under- and over- estimated respectively.

Results from the Easter Bush site indicate that canopy and stomatal conductance are, in general, over-estimated by a factor of 2 at Easter Bush. The measurements indicate that the non-stomatal component is controlled by factors other than LAI and as such is not well reproduced by the model. It is envisaged that further analysis and tuning of the model will improve its performance with these datasets. It was concluded that extensive datasets of total and stomatal ozone deposition fluxes are required to improve and validate the model, particularly for the non-stomatal deposition term. A more detailed summary of this component of the research programme can be found in Annexe 1.

Figure 2.2 Diurnal cycle of hourly measured and modelled ozone deposition velocity over a). sugar beet on the 18th of July 2000 and b) oats on the 22nd June 200 at Sutton Bonnington.

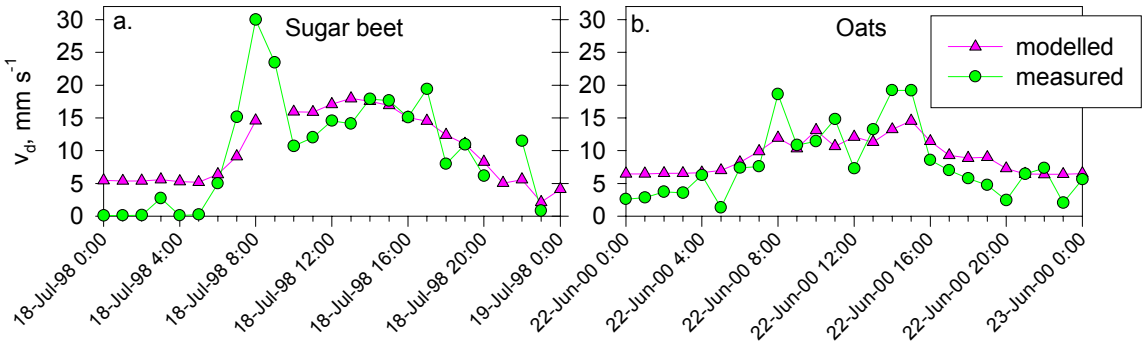

## 2.3 Mediterranean Ecosystem Comparisons

### Introduction

The EMEP deposition module has been evaluated against observations of total ozone flux and stomatal conductance for a number of different ecosystem types representative of central and northern European locations (e.g. Emberson et al. 2000a; Tuovinen et al., 2001a and 2001b; Coyle et al, submitted). These have generally shown that the model performs well, although improvements in the model predications could be achieved through "tuning" the model parameterisation for local conditions. However, the module has not been as extensively tested under Mediterranean conditions with only one comparative study (Tuovinen et al., in press) having been conducted to date for wheat growing in Italy. It is imperative that further evaluations should be performed, firstly since the model should be tested under all European climate types and secondly, since these regions are prone to co-occurring elevated ozone concentrations and high soil and atmospheric water deficits. As such, these conditions may lead to large differences in the accumulation of exposure versus flux-based indices that may be especially relevant to European emission abatement formulation.

### Data description

The Californian vineyard dataset (Massman & Grantz, 1995; Pedersen et al. 1995) was offered for use in evaluation of the EMEP ozone deposition model at the UN/ECE workshop held in Harrogate, June 2002 by Dr. Bill Massman. Although these data were obtained under North American conditions it was considered that the semi-arid climate of the study area is similar to Mediterranean conditions and hence could provide important information as to how well the model may perform under such climatic conditions.

The data set used in this study was collected as part of the California Ozone Deposition Experiment (CODE) during July and August of 1991. Measurements were taken at a grape vineyard site (*Vitis vinifera* L. cv. Thompson seedless) located in the San Joaquin Valley in California (36˚51′36″N,120˚6′7″W). There was no precipitation during the study period, but the plants had been irrigated before the start of the experiment. The sky remained virtually cloud free for the duration of the investigation. There was almost no growth in the vineyard plants, since they had reached their maximum vegetative state (LAI = 3.4, vegetation height = 1.7m)

Flux data for ozone, heat, water vapour, $CO_2$ and momentum were measured half hourly using eddy covariance. Other half hourly measurements made include incoming solar radiation, net radiation, soil heat flux, atmospheric temperature, atmospheric humidity, horizontal wind speed and direction, atmospheric pressure, soil temperature, infrared surface and foliage temperature, atmospheric ozone concentration and readings from dew sensors. In addition, daily measurements of volumetric soil water content and some diurnal courses of leaf conductance to water vapour were made. More detailed site measurement and data descriptions for the CODE 91 experiment are given in Massman et al. (1994) and Pederson et al. (1995).

## Model Description

The basic stomatal flux and total ozone deposition model that is evaluated here using the CODE 91 data has been described previously in an EMEP note (Emberson et al., 2000a). Some modifications to this model have been made and are described as follows:-

i). The calculation of stomatal conductance ($g_{sto}$) is made using equation [2.3.1]. This has been modified from that described in the EMEP note by allowing the $f_{light}$ relationship to effectively completely shut the stomata.

$$g_{sto} = g_{max} * f_{phen} * f_{light} * \max\{f_{min}, (f_{temp} * f_{VPD} * f_{SWP})\} \quad [2.3.1]$$

ii). The calculation of $f_{temp}$ has been modified to an asymmetrical relationship. This allows for differential $g_{sto}$ sensitivity to changing temperature around the temperature optimum and the new formulations are described in equation [2.3.2].

$$f_{temp} = \max \{f_{min}, [(T-T_{min}) / (T_{opt}-T_{min})] * [(T_{max}-T) / (T_{max}-T_{opt})]^{bt}\} \quad [2.3.2]$$

where T is the air temperature in $^{o}$C, $T_{min}$ and $T_{max}$ are the minimum and maximum temperatures at which stomatal closure occurs to $f_{min}$, $T_{opt}$ is the optimum temperature and bt is defined as:

$$bt = (T_{max}-T_{opt}) / (T_{opt}-T_{min})$$

iii). A new method has been used to estimate the canopy radiative transfer following the suggestions of Zhang et al. (2001). Zhang et al. (2001) found that the use of the Norman (1982) canopy radiative model introduced potential errors since the formulae of Norman give overestimations of the photosynthetically active radiation (PAR) received by the shade leaves ($PAR_{shade}$) within canopies when LAI exceeds 2 $m^2/m^2$. A similar concern was reported from work performed under a previous Defra funded research contract (EPG 1/3/104). Zhang et al. (2001) suggest a new formula for $PAR_{shade}$ (see equation 2.3.3) that is more suitable for "big-leaf" canopy stomatal resistance models since it takes into account the vertical visible radiation profiles received by shaded leaves.

$$PAR_{shade} = I_{diff} * \exp(-0.65*LAI^{1.5}) + 0.07 * I_{dir} * (1.1-0.1* LAI) * \exp(-\sin\beta) \quad [2.3.3]$$

Where $I_{diff}$ and $I_{dir}$ are diffusive and direct PAR respectively and $\sin\beta$ is the solar variation (calculated as a function of latitude and time of year).

## Vineyard parameterisation

The stomatal and deposition model parameterisation described in the EMEP note were collected from literature searches conducted pre-1997. Hence, it was considered appropriate to conduct a new literature search to "up date" the parameterisation using as recently published data as available. The methods used to derive the grapevine $g_s$ parameterisation were the same as those applied previously as described in Emberson (1997). The new parameterisations are shown in Figures 2.3.1 and 2.3.2 and were used to construct the "EMEP literature" model (model 1 in Table 2.3.1). Alternative model variations in both formulation and parameterisation were also developed to "tune" the model to the local CODE 91 data (both in terms of gs and total ozone deposition measurement data). These variants are described in Table 2.3.1 with model runs being tested against both a). gs data and b). total $O_3$ deposition data.

**Table 2.3.1** Model parameterisation and variants used for evaluation against the CODE data.

| Model | 1 **EMEP Literature** | 2 **EMEP Local** | 3 **Local $\Delta f_{light}$ [1]** | 4 **Local $\Delta f_{light}$ [2]** | 5 **Local $\Delta f_{light}$ [3]** | 6 **EMEP Local_ SWP** | 7 **Local $\Delta f_{light}$ [2]_ SWP** | 8 **EMEP Local** | 9 **Local $\Delta f_{light}$ [2]** |
|---|---|---|---|---|---|---|---|---|---|
| **Formulation*** | **a** | **a** | **a** | **a** | **a** | **a** | **a** | **b** | **b** |
| **$g_{max}$ (mmol $O_3$ $m^{-2}$ $s^{-1}$ (P)** | **230** | **315** | **315** | **315** | **315** | **315** | **315** | **315** | **315** |
| **$f_{min}$** | **0.05** | **0.03** | **0.03** | **0.03** | **0.03** | **0.03** | **0.03** | **0.03** | **0.03** |
| **a_light** | **0.004** | **0.0022** | **see [1]** | **see [2]** | **see [3]** | **0.0022** | **see [2]** | **0.0022** | **see [2]** |
| **$T_{max}$** | **39** | **40** | **40** | **40** | **40** | **40** | **40** | **40** | **40** |
| **$T_{opt}$** | **29** | **29** | **29** | **29** | **29** | **29** | **29** | **29** | **29** |
| **$T_{min}$** | **12** | **13** | **13** | **13** | **13** | **13** | **13** | **13** | **13** |
| **VPD_max** | **1.3** | **>2.4**** | **>2.4**** | **>2.4**** | **>2.4**** | **>2.4**** | **>2.4**** | **>2.4**** | **>2.4**** |
| **VPD_min** | **4.3** | **>2.4**** | **>2.4**** | **>2.4**** | **>2.4**** | **>2.4**** | **>2.4**** | **>2.4**** | **>2.4**** |
| **SWP_max** | **-0.35** | **>-1.2**** | **>-1.2**** | **>-1.2**** | **>-1.2**** | **-1.6** | **-1.5** | **>-1.2**** | **>-1.2**** |
| **SWP_min** | **-0.9** | **>-1.2**** | **>-1.2**** | **>-1.2**** | **>-1.2**** | **-2.0** | **-2.0** | **>-1.2**** | **>-1.2**** |

* Two different formulations for the calculation of $g_s$ were used:-

a $g_s = g_{max} * f_{pot} * f_{light} * \max(g_{min}, (f_{temp}*f_{VPD}*f_{SWP}))$

b $g_s = \max(g_{max}*f_{pot}*f_{light}*\max(g_{min}, (f_{temp}*f_{VPD}*f_{SWP})), 0.1*g_{max})$

** The $g_s$ data only suggest that the threshold for VPD and SWP influence on gs have not been reached under the measurement conditions. As such, these parameters were set as if to 1 i.e. not limiting, for the model runs performed using local parameterisation.

[1] $f_{light} = (0.00038*PAR-0.0313)+0.19$

This function is derived from a linear regression of measured gs with PAR

[2] $f_{light} = 1-e^{-\alpha*PAR/PARmax)} / 1-e^{-\alpha}$

This function describes $f_{light}$ as a negatively concave relationship where $\alpha = -0.6$ and $PAR_{max} = 2000$.

[3] $$f_{light} = \left[\frac{1-e^{-\alpha\alpha AR/PARmax}}{1-e^{-\alpha}}\right]\left[\frac{1+\beta e^{-\alpha}}{1+\beta e^{-\alpha PAR/PARmax}}\right]$$

This function describes $f_{light}$ as a sigmoidal relationship where $\alpha = -0.6$ and $PAR_{max} = 2000$.

**Figure 2.3.1** The mean (solid line), median (broken line) and range of $g_{max}$ values from different observations of $g_s$ for grapevine. $g_{max}$ units are in mmol $O_3$ $m^{-2}$ $s^{-1}$ on a projected leaf area basis.

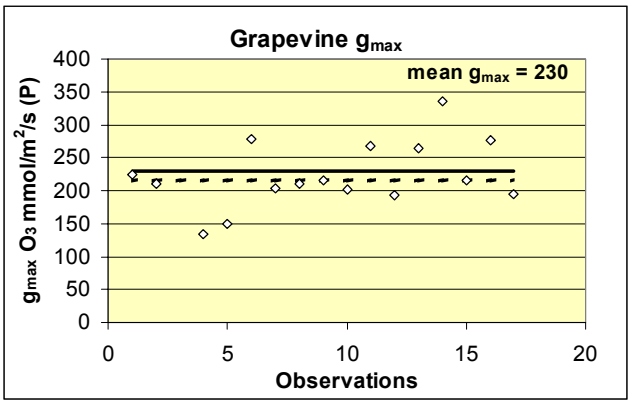


**Figure 2.3.2** Figures describing the EMEP $g_s$ relationships $f_{light}$, $f_{temp}$, $f_{VPD}$ and $f_{SWP}$ for grapevine (red lines) estimated from published data (symbols).

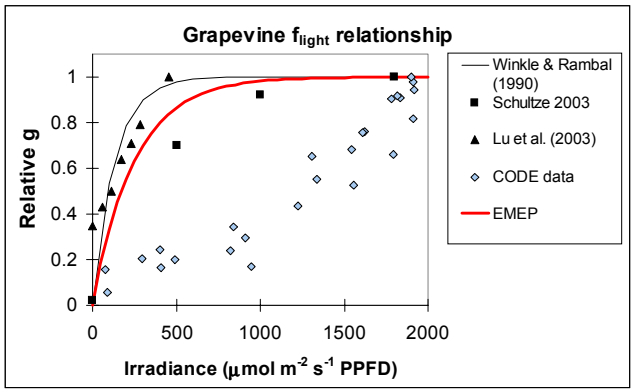


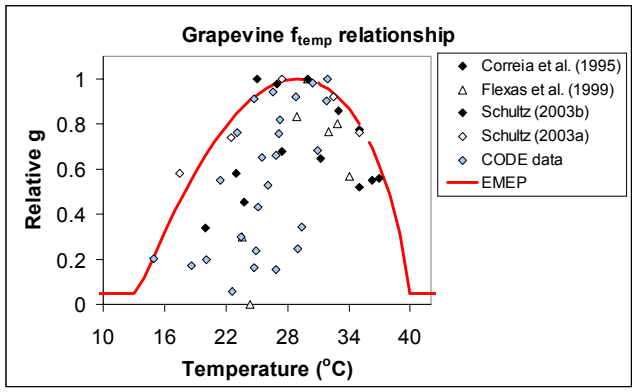


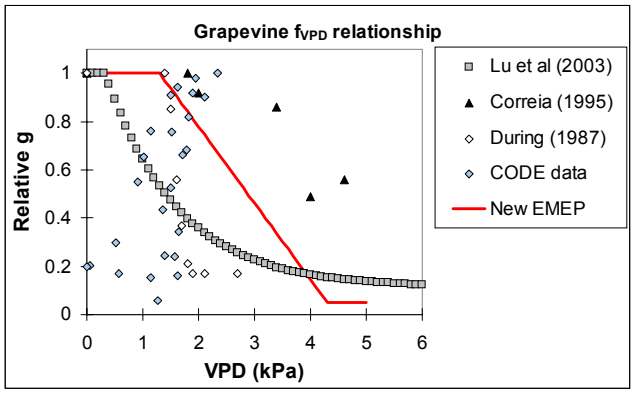


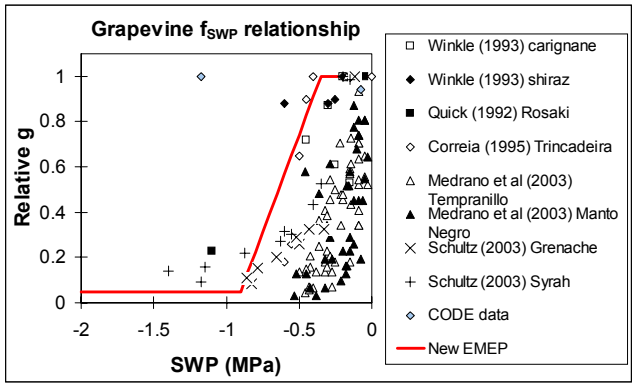

## Derivation of environmental parameters

To enable application of the stomatal conductance and deposition models it was necessary to derive certain environmental parameters from the environmental data collected during the experimental campaign; for example, estimates of direct and diffuse PAR are necessary as input to the canopy radiative transfer model (see equation 2.3.3). The method of Weiss and Norman (1985) was used for this derivation. Measurements of soil water potential were made only for one soil depth (approx. 8cm). As such, these measurements do not give an indication of the soil water status over the whole rooting depth (which would normally be expected to extend to a depth of at least 1 m for vineyards). In view of this it was assumed that the soil water status was not limiting $g_s$ for the initial model runs (i.e. tests of models 1 to 5 and 8 to 9; see Table 2.3.1 for details). However, the soil water potential data was used to "tune" the model when comparing the measured against modelled ozone deposition data. This allows some indication of the effect of an inferred integrated soil water potential on $g_s$ that can then be related to the parameterisation extracted from the literature.

## Results

The different formulations and parameterisations described in Table 2.3.1 were used to model gs and ozone deposition. These modelled values were evaluated against measured data using linear regression. The results of these comparisons are shown in Table 2.3.2.

Table 2.3.2 Linear regression statistics (forced through zero) between modelled (using different model variants) and measured values for $g_s$ and ozone deposition data.

| | gs | | Ozone deposition | |
|---|---|---|---|---|
| Model variant | **$R^2$** | **slope** | **$R^2$** | **slope** |
| Night-time gs = 0 | | | | |
| 1 **EMEP Literature** | **0.4769** | **0.9431** | **0.7363** | **0.5769** |
| 2 **EMEP Local** | **0.6297** | **0.7524** | **0.7575** | **0.5148** |
| 3 **Local St. line $f_{light}$** | **0.8655** | **0.9886** | **0.7868** | **0.5568** |
| 4 **Local Neg. concavity $f_{light}$** | **0.9093** | **1.009** | **0.7915** | **0.8037** |
| 5 **Local Sigmoidal $f_{light}$** | **0.908** | **1.0007** | **0.7922** | **0.8084** |
| SWP tuning: Night-time gs =0 | | | | |
| 6 **Local St. line_SWP** | **0.8655** | **0.9886** | **0.7868** | **0.5568** |
| 7 **Local Neg. concavity _SWP $f_{light}$** | **0.9093** | **1.009** | **0.7925** | **0.8063** |
| Night-time gs = 0.1 $g_{max}$ | | | | |
| 8 **EMEP Local** | **0.6297** | **0.7524** | **0.7275** | **0.678** |
| 9 **Local Neg. concavity $f_{light}$** | **0.9093** | **1.009** | **0.6817** | **0.9061** |

Table 2.3.2 shows that the model predictions can be improved by altering both the parameterisation and formulation of the EMEP deposition model. In summary, the changes that were most influential involved the parameterisation of $g_{max}$ (with model predictions being improved when using the local $g_{max}$ parameterisation) and the $f_{light}$ formulation (predictions being improved as the $f_{light}$ relationship is closer to a straight line). Small improvements to the modelling were also made by introducing a limiting $f_{SWP}$ function, derived by tuning the overall ozone deposition model results to more accurately reflect the measured data.

For the purposes of assessing the performance of the EMEP deposition model it is useful to look at some of the results obtained by selected model runs in a little more detail. Firstly, it is important to assess just how well the EMEP deposition model performs when using parameterisation and formulation obtained from the literature since this represents the true predictive capabilities of the existing deposition model. Figure 2.3.3 shows the diurnal gs and total ozone flux values modelled using the EMEP literature parameterisation. In comparison Figure 2.3.4 shows the same using local data to parameterise the EMEP model (i.e. adjusted $g_{max}$ and f relationships). Both modelled datasets are shown with the corresponding measured gs data as available throughout the study period. It is clear from both the $g_s$ $R^2$ values and diurnal profiles that the local parameterisation improves both the prediction of $g_s$ (from an $R^2$ value of 0.4769 to 0.6297) and total ozone flux (from an $R^2$ value of 0.7363 to 0.7575). This is largely due to the adjustments made to $g_{max}$ (which was increased from 230 to 315 mmol $O_3$ $m^{-2}$ $s^{-1}$) as evident from the gs diurnal profiles showing that the local model parameterisation gives modelled gs values of the same magnitude as the measurements. In both cases the model is consistently and significantly over-predicting total ozone deposition, with the slopes of the linear regressions averaging around 0.55.

Figure 2.3.4 shows that although the altered $g_{max}$ value improves the prediction of the highest $g_s$ values, the diurnal profile is still not accurately predicted. Reasons for this were investigated by plotting measured gs against each environmental parameter (i.e. irradiance, temperature and VPD). From this it was evident that the EMEP formulation used to describe $f_{light}$ was not appropriate since $g_s$ seemed to increase with irradiance in a linear rather than convex exponential fashion (see Figure 2.3.5). To test this hypothesis a number of different $f_{light}$ relationships were constructed (see Figure 2.3.5). A straight line relationship (derived by performing a linear regression on the $g_s$ data plotted against irradiance) representing the simplest formulation option. Two rather more complex formulations, a negatively concave and sigmoidal relationship (both of which were similar in shape), were also tested. Each of these were individually substituted for the existing $f_{light}$ relationship in the deposition model and compared with the observed data (see Table 2.3.2).

Figure 2.3.3 Comparisons between modelled and measured diurnal gs and total ozone flux. Modelled values are obtained using a). the EMEP literature parameterisation

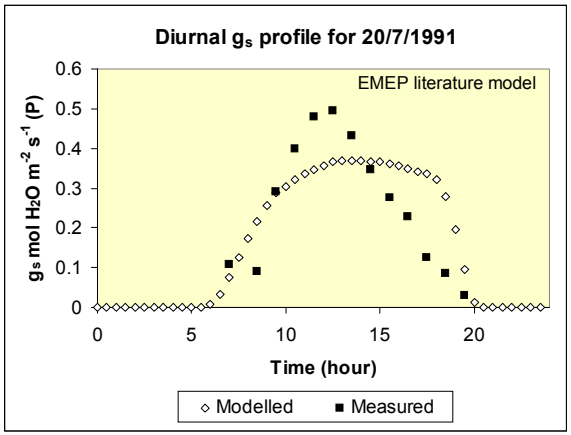


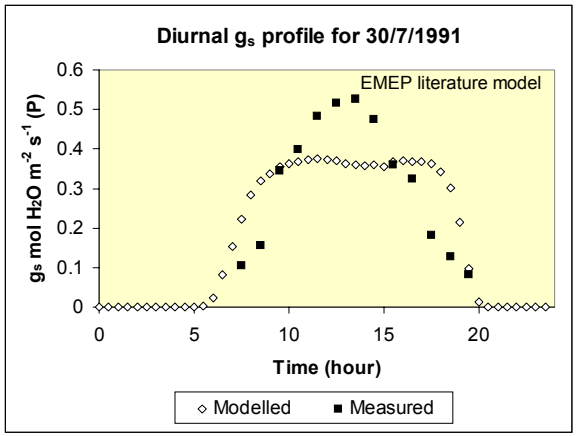


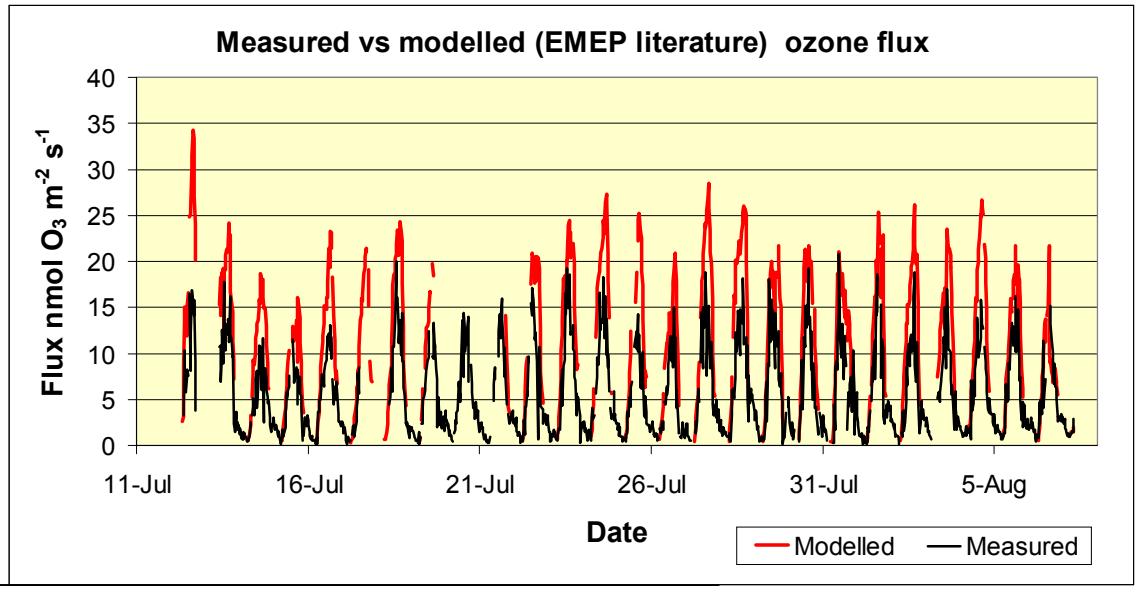

Figure 2.3.4 Comparisons between modelled and measured diurnal gs and total ozone flux. Modelled values are obtained using the EMEP local parameterisation.

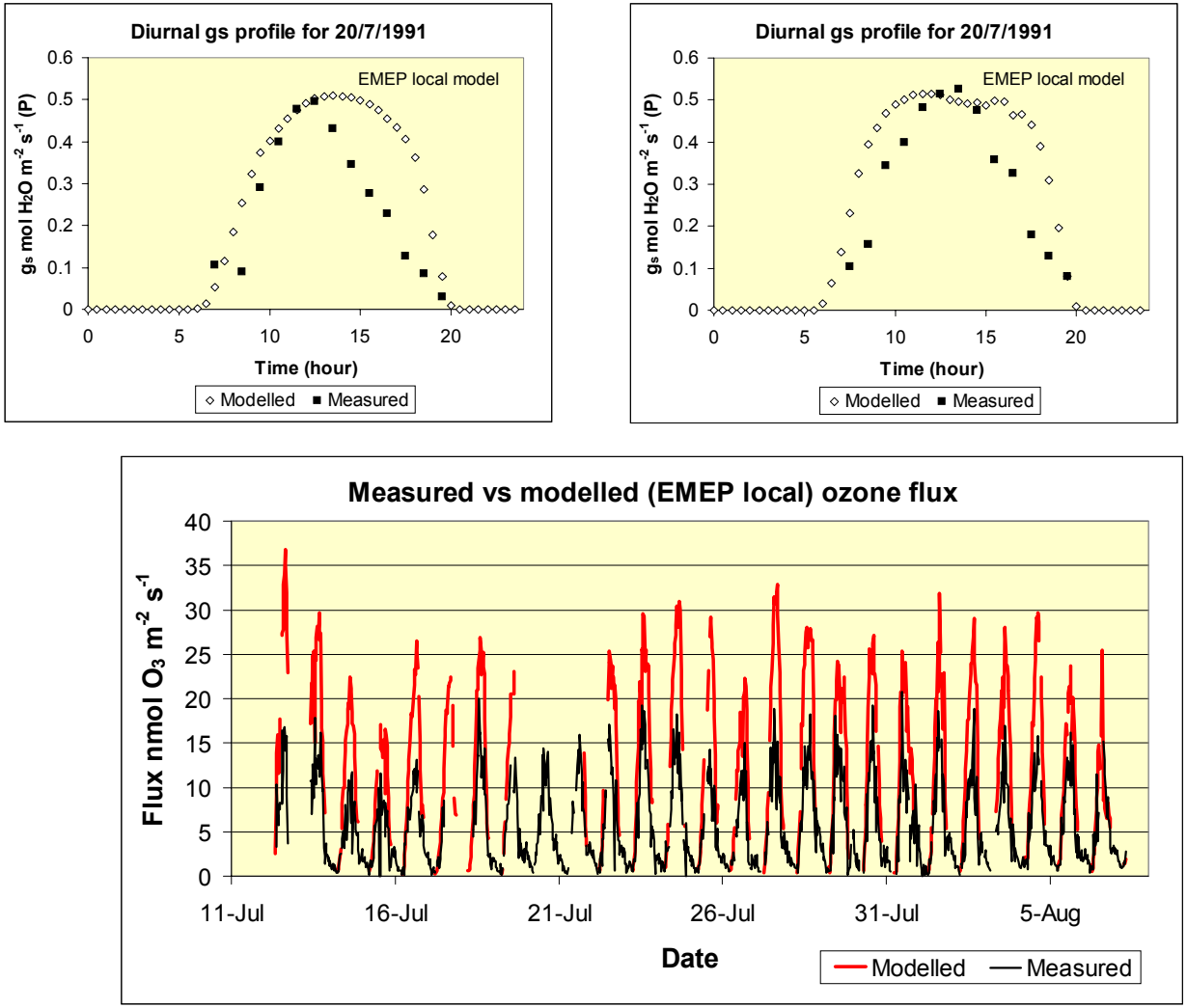

Figure 2.3.5 Alternative $f_{light}$ relationships used within the deposition model.

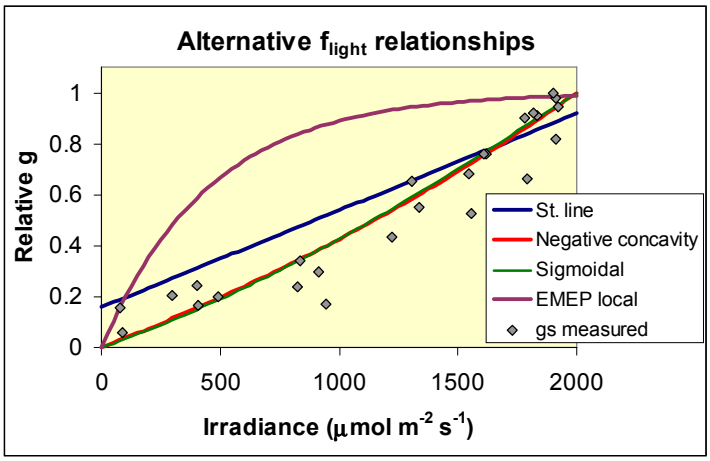


The more complex $f_{light}$ formulations significantly improved the gs model predictions (giving $R^2$ values of between 0.909 and 0.908) with subsequent improvements in the ozone flux models predictions (with $R^2$ and slope values of approximately 0.79 and 0.8 respectively). The negatively concave $f_{light}$ relationship resulted in the greatest model improvement. The "simpler" straight line relationship improved the $g_s$ model predictions but did little to improve the overall ozone deposition model predictions with regression slope values of around 0.55 due to consistent over-prediction.

Figure 2.3.6 shows the improvements in the model predictions of total ozone flux that were achieved using the negatively concave $f_{light}$ relationship. However, the average diurnal soil water potential values plotted in Figure 2.3.6 suggest that the reduced soil water status at the beginning of the experimental period may be influencing ozone deposition since the model consistently over-predicts deposition during this period. Most likely, the reduction in $g_s$ is caused by a soil water deficit. To investigate this further the predictive capabilities of the model were "tuned" by altering SWP_max and SWP_min until the optimum $R^2$ and slope values were obtained. The results of this "tuning" are shown in Figure 2.3.7, in which the circle identifies the period when ozone deposition was reduced by increasing the gs model sensitivity to SWP. It should be noted that this "tuned" SWP parameterisation (SWP_max = -1.6 MPa; SWP_min = -1.9 MPa) would be expected to be lower than the literature derived parameterisation (SWP_max = -0.35 MPa and SWP_min = -0.9 MPa) since the former represents the SWP in only the upper soil layer; which will dry more quickly than the soil over the whole of the rooting depth. It is the SWP of the entire rooting depth to which the literature $f_{SWP}$ should be applied.

Table 2.3.1 also describes model formulations used to simulate night-time stomatal opening. Although $g_s$ measurements were only taken during daylight hours, a number of recent papers (e.g. Massman & Grantz, 1995) have suggested that some stomatal flux occurs during the night-time. Since the capacity of the leaves to detoxify absorbed ozone dose tends to be reduced during the night, such stomatal opening may have significant effects on ozone damage. Model runs were performed using the model variants "EMEP local" and "Local $\Delta f_{light}^2$" but on both occasions the $R^2$ values for the measured versus modelled data were not as good as when assuming no night-time $g_s$ (see Table 2.3.2). However, this should not necessarily be interpreted as there being no night-time $g_s$, since it may be that the magnitude of nigh-time gs varies.

Figure 2.3.6 Comparisons between modelled and measured diurnal gs and total ozone flux. Modelled values are obtained using local parameterisation with the negatively concave $f_{light}$ formulation. Corresponding soil water potential values are also recorded.

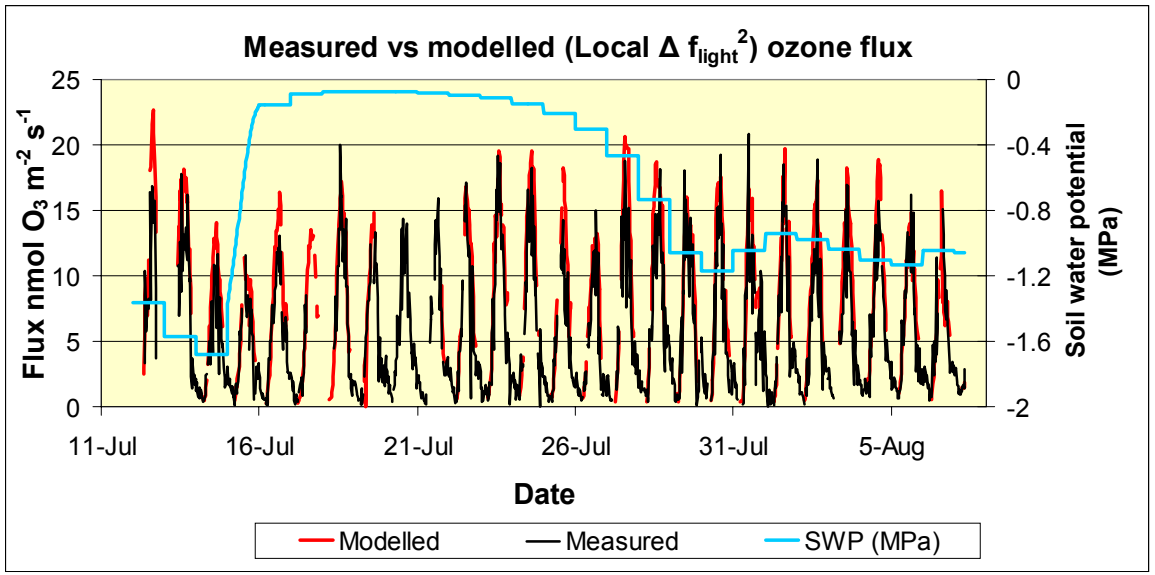

Figure 2.3.7 Comparisons between modelled and measured total ozone flux. Modelled values are obtained using local parameterisation with the negatively concave $f_{light}$ formulation and "tuning" the ozone deposition model values by altering the $g_s$ sensitivity to soil water potential. SWP_max = -1.6MPa; SWP_min = -1.9MPa.

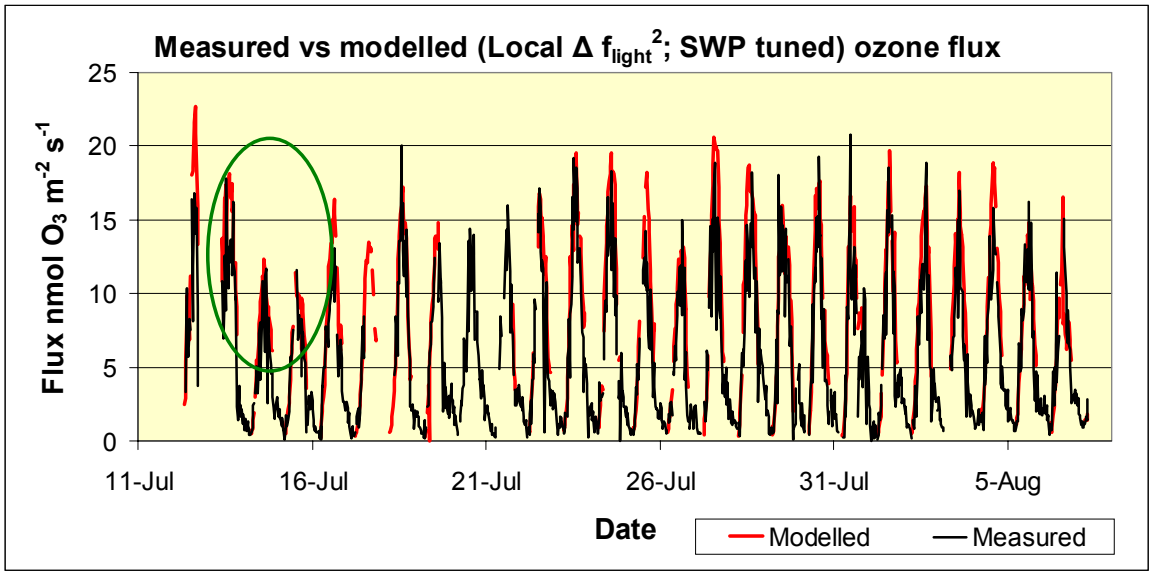


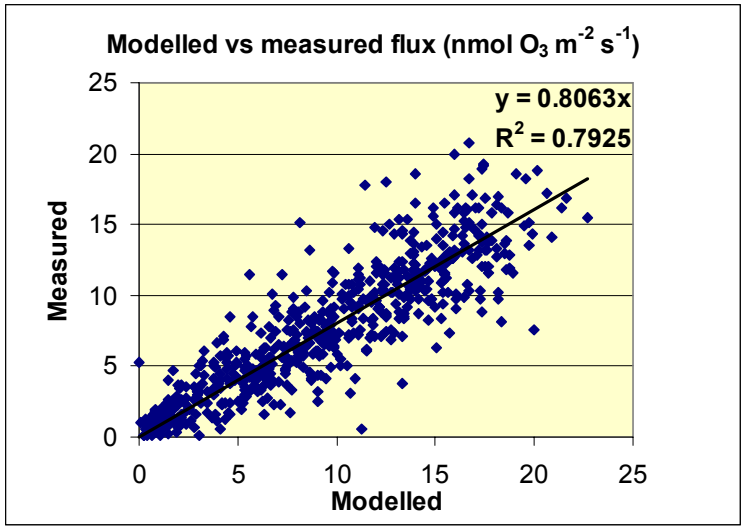

## Discussion / conclusion

In summary, the results have shown that when the stomatal and deposition models are formulated and parameterised according to local data for vineyards, they are capable of explaining 90 and 79% of the variation in gs and total ozone deposition respectively. The key component of the existing EMEP deposition model that required both re-formulation and –parameterisation was the $f_{light}$ relationship. This was due to the rather insensitive response of the $g_s$ of Californian grapevine to irradiance. The CODE 91 data broadly agree with the $f_{temp}$ relationship derived from the literature. The literature derivation of $f_{VPD}$ was extremely uncertain with the collated datasets showing quite different gs responses to increased VPD. As such, it is not surprising that this relationship needed to be adjusted to improve the predictive capabilities of the deposition model. The $f_{SWP}$ relationship could not be evaluated since the necessary integrated root depth SWP parameter was not available; however, altering the SWP function in relation to the surface layer SWP value did improve the model's performance under especially dry conditions. The $g_{max}$ value was also important in determining the range of $g_s$. Figure 2.3.1 and Table 2.3.4 show that $g_{max}$ values derived from the literature range from 135 to 336 mmol $O_3$ $m^{-2}$ $s^{-1}$. The local $g_{max}$ value of 315 mmol $O_3$ $m^{-2}$ $s^{-1}$ for the Californian grapevine is towards the higher end of this range and explains why using local parameterisation again improved the model predictions.

A key question is whether these new Californian gs data should be used to drive modifications of the EMEP model. The data have already been included in the $g_{max}$ derivation (see Table 2.3.4) and it is clear that the data also confirm the literature derived $f_{temp}$ relationship. However, key factors are the $f_{light}$ and $f_{VPD}$ relationships. Should these be modified according to the CODE 91 data? If the answer is yes, then the new $f_{light}$ formulation would mean that vineyards would have to be treated as a separate case. Ideally, additional data will become available to confirm or reject the changes made to the best performing model described here; this should occur given that new datasets which are available for similar model evaluation exercises have already been identified.

# 3. Improvements to the formulation and parameterisation of the $O_3$ stomatal flux model

## 3.1 Revision of the ozone stomatal flux model formulation

The results of model evaluations, such as those described in Section 2, and of other scientific discussions and dialogues, a number of changes in the model formulation have been suggested over the past three years to improve the deposition model compared to that described in the EMEP Note of 2000 (Emberson et al. 2000). These changes (and the reasons for the alterations to the formulations) have been documented in the progress reports submitted to Defra over the duration of this contract. Full details will not be repeated here. However, a summary of the alterations that have been made is provided in Table 3.1.1 and the following text describes the evolution and rationale of each of the suggested modifications. It is also worth noting that the notation commonly used to describe the model components has become rather diverse, since the model has been used by a large number of scientists across Europe. The recent revision of the Mapping Manual (in April 2003) (see Section 7.3 of this report) provided a forum for a number of interested scientists across Europe, together with members of our consortium, to agree on a common notation for flux modelling. This will be used in this and subsequent reports, and details are given in Annexe 2 of this Report.

### Growing season

For two species (wheat and potato), representing the temperate crops and root crops land-cover types respectively, thermal time models have been established and passed through peer review via the formulation of the revision to the UN/ECE Mapping Manual. Details of these models, as described in the Mapping Manual, are given briefly below for both wheat and potato. The methods employed rely on phenological growth models or local agricultural statistics/information to predict the timing of growing season in the absence of observational data describing actual growth stages.

**Table 3.1.1** Summary of suggested alterations to the EMEP deposition model with rationale that have been made over the duration of the project.

| Model component | Alteration | Rationale |
|---|---|---|
| **Growing season** | Incorporation of thermal time models to estimate start and end of growing seasons | To incorporate variations in annual cumulative temperature in predictions of $g_{sto}$. Such information can also be used in combination with LAI to improve total deposition estimates |
| **Canopy $g_{sto}$** | Include leaf populations when scaling from leaf to canopy conductance using Leaf Area Index for crop cover types (see Tuovinen et al. sub) | To improve the modelling of canopy $g_{sto}$ for wheat |
| **$f_{phen}$** | Modification of $f_{phen}$ calculation for temperate needle leaf species (see Weiser & Emberson, in press) | To improve the seasonal description of $g_{sto}$ |
| **$f_{light}$** | 1). Flexibility in the location of $f_{light}$ within the $g_{sto}$ formulation<br><br>2).Change to the function describing $f_{light}$ for vineyards (from exponential to almost a straight line function) | 1). Allows night-time stomatal uptake to be modelled for species as desirable.<br>2) Improved model performance for Californian vineyard site (see this report) – this should be tested on other vineyard datasets before a change in the EMEP model for this cover type is recommended |
| **$f_{temp}$** | Change to the function describing $f_{temp}$ | Allows for the increase and decrease in stomatal conductance around the temperature optimum to vary in sensitivity |

*Wheat*

Start of Growing Season: Typical sowing dates for *spring wheat* are given in Table 3.1.2. From the sowing date, the date of emergence can be estimated based on the temperature sum (above 0 $^{o}$C) for different sowing depths (Hodges & Ritchie, 1991). For this cover-type, an average sowing depth of 3 cm is assumed and the temperature sum required for emergence is 70 $^{o}$C days. For *winter wheat*, growth restarts after the winter when temperature exceeds 0 $^{o}$C.

End of Growing Season: For both *spring and winter wheat*, the end of the growing season can be estimated using a temperature sum value of 1775 $^{o}$C days calculated from emergence or start of re-growth as appropriate.

*Potato*

Start of Growing Season: For potato it is necessary to identify plant emergence, which normally takes place one week to ten days after sowing of the potatoes. The sowing date varies to a considerable extent across Europe. However, in the EU funded research programme CHIP, which investigated the effects of ozone and other stresses on potato, the plant emergence was obtained on average on day of year 146, with a variation from day 135 at southern and most western European sites to day 162 in Finland.

End of Growing Season: For *potato*, the end of the growing season can be estimated using a temperature sum value of 1130 $^{o}$C days calculated from emergence.

Table 3.1.2 Observed sowing dates for spring wheat in Europe [1)]

| Region | Spring wheat | |
|---|---|---|
| | Range | Default |
| **Northern Europe** | | |
| Finland | 1-30 May | 30 May |
| Norway | 1-20 May | 20 May |
| Sweden | 1-20 April | 20 April |
| Denmark | 1 Mar-20 Apr | 20 March |
| Continental Central Europe | | |
| Poland | 1-20 Apr | 10 April |
| Czech Republic | 10-30 Apr | 20 April |
| Slovakia | 10-30 Apr | 20 April |
| Romania | - | |
| Hungary | - | |
| Germany | 10 Mar-10 Apr | 1 April |
| Atlantic Central Europe | | |
| UK | 20 Feb-20 Mar | 10 March |
| The Netherlands | 1-30 Mar | 15 March |
| France | 1 Mar-10 Apr | 20 March |
| Mediterranean Europe | | |
| Bulgaria | - | |
| Portugal | 20 Jan-10 Mar | 10 February |
| Spain | 1-28 Feb | 10 February |
| Italy (soft and durum wheat) | - | (not grown) |

[1)] According to Broekhuizen (1969)

### Canopy $g_{sto}$

An assessment of the suitability of the ozone deposition and stomatal flux model for wheat growing under Mediterranean conditions was completed earlier this year and highlighted the need to re-formulate the methods to up-scale from the leaf to the canopy. This comparison made use of the recent ozone flux data reported by Gerosa et al. (2003). These data originated from a micrometeorological study conducted in an extensive wheat (*Triticum aestivum* cv. Bilancia) field in Northern Italy in May–June 2001. The measurements cover the whole grain filling period from anthesis to harvest, but in the analyses presented here (and described further in Tuovinen et al. (submitted)) only the first part of the growing period (when the observed soil water content was close to field capacity and the deposition velocities were highest) was considered. The measurement data include the inferred stomatal conductance for the canopy.

Model runs were performed using the original (or default) version of the ozone deposition and stomatal flux model (Emberson et al., 2000b). These indicated that the EMEP module systematically over-predicted both the canopy stomatal conductance and deposition velocity (Figure 3.1.1). The over-prediction of stomatal conductance was considered to be related to using flag-leaf data as representative of the whole canopy. Therefore, a revised version was developed which modelled the life cycles of six main leaves (leaf populations) of wheat. Based on data presented by Araus et al. (1986), each leaf was assigned a different emergence date, age modifier ($f_{age}$) and leaf area index. The growing season length remained at 92 days, as in the original version, but the leaves were assumed to emerge at 9-day intervals. The dependence of $g_{max}$ on the leaf insertion level was included in the $f_{age}$ calculation, which attains a maximum value ranging from 0.7 (first leaf) to 1 (flag leaf) in 4 days. Leaf senescence takes 45 days. The maximum leaf area index varies from 0.6 (first leaf) to 1.2 (flag leaf) and is reached when $f_{age}$ is at its maximum. For all leaves, the maximum LAI lasts for 20 days,

after which the green area is reduced to zero in 10 days. After this, the remaining (senescent) leaf area is reduced to zero in 30 days.

Figure 3.1.1 The measured and modelled averaged diurnal cycles of stomatal conductance (a), total surface conductance (b) and deposition velocity (c) at Comun Nuovo. Modelled results are based either on the original EMEP parameterisation or on the revised parameterisation, including different leaves

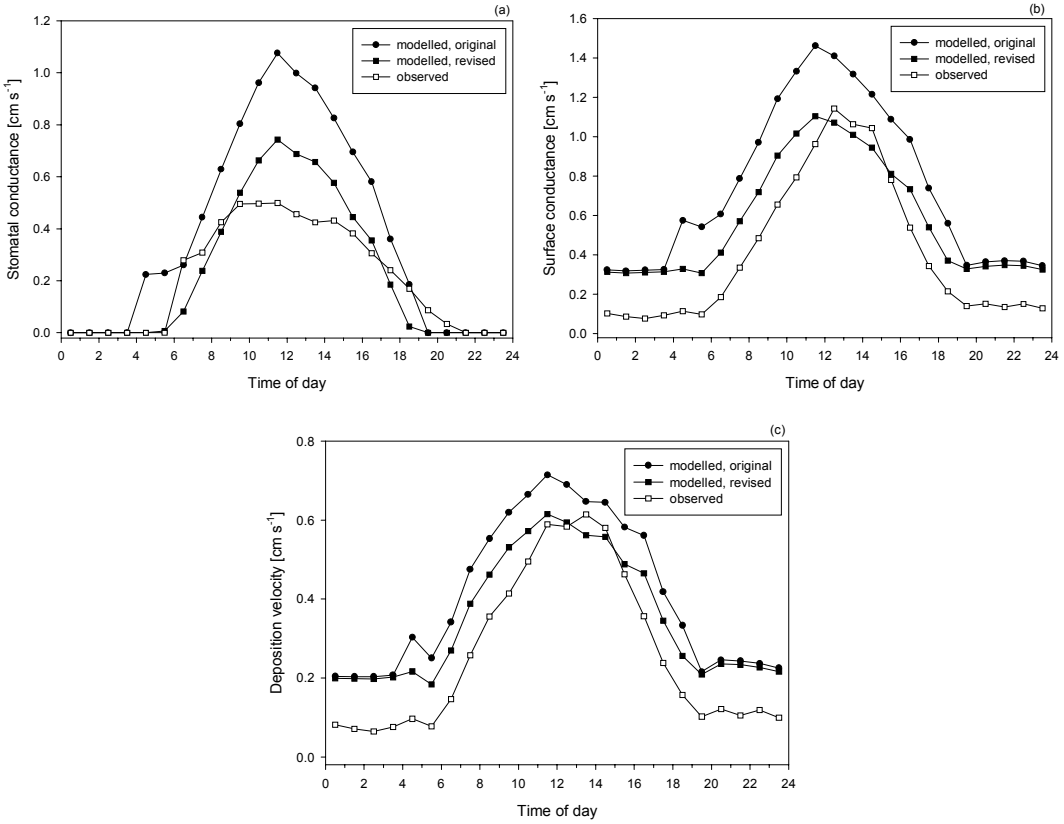


The canopy-scale conductance was derived by combining the status of the different leaf populations as described in equation [3.1.1].

$$G_{sto} = g_{max} \cdot F_{age} \cdot f_{env}, \qquad [3.1.1]$$

where $F_{age}$ is the effective canopy-scale age factor calculated as a sum of $f_{age}$· LAI over the green areas of the six leaves. For the model implementation, the resulting temporal development of the total LAI and $F_{age}$ were estimated by linear segments. While the assumptions described above result in the same maximum total LAI of 5 as in the original model version, $F_{age}$ is always smaller than this. This up-scaling procedure effectively means that it is possible to differentiate between the green (non-senescent) leaf area and the total leaf area, as in the models of Grünhage et al. (1999) and Bassin et al. (submitted). As an additional modification to the default model, the minimum stomatal conductance was set to zero.

As the lower leaves have a lower maximum conductance and are more senescent than the flag leaf during the observation period, the new parameterisation gives lower canopy stomatal conductance than the default version (Figure 3.1.1). Despite this reduction, the revised model still tends to over-predict the midday values of $G_{sto}$. Another discrepancy in the average diurnal cycle is that the parameterisation limits the modelled $G_{sto}$ too efficiently at low light levels. The daily maximum of the

deposition velocity is predicted accurately by the revised model, but except for these midday hours, there is a systematic difference between the model results and observations (Figure 3.1.1c). This pattern is even more apparent in the total surface conductance (Figure 3.1.1b).

As the total surface conductance is significantly overestimated during the night, it seems likely that the systematic differences in both total surface conductance and deposition velocity are related to the parameterisation of the non-stomatal conductance components. The nocturnal canopy conductance values would indicate that non-stomatal conductance is overestimated, but the situation is reversed during the daytime period when $G_{sto}$ was overestimated. This means that the residual non-stomatal conductance exhibits a diurnal cycle with higher values during the daytime, as found by Gerosa et al. (2003). Comparison of Figures 3.1.1a and 3.1.1b reveals that the hourly averaged non-stomatal conductance varies from the nocturnal level of about 0.1 cm $s^{-1}$ to the maximum value of 0.67 cm $s^{-1}$, while the corresponding range is 0.30–0.39 cm $s^{-1}$ for the values obtained from the revised model. Thus the EMEP module has been parameterised to allow for a relatively large non-stomatal deposition, agreeing with the conclusions of Gerosa et al. (2003). However, the module lacks the diurnal variation observed in this component. It would be easy to incorporate such diurnal variability, but given the diversity of contributing processes the data are considered to be too limited to derive a generalised parameterisation at present.

In summary, the new up-scaling method developed and tested against for wheat data from Northern Italy has partly removed the overestimation of the stomatal conductance observed when using the standard parameterisation. The deposition velocity at midday was predicted well, but the partitioning of the flux between the stomatal and non-stomatal components was not consistent with measurements, which suggest a diurnal cycle in the non-stomatal conductance. A more detailed study based on these data is recommended. This should address non-stomatal deposition, which forms a significant part of the total flux, and the drier part of the growing season.

### Coniferous phenology function ($f_{phen}$)

Estimates of $g_{sto}$ for individual leaves or needles need to be scaled according to LAI values to estimate whole canopy $g_{sto}$. This requires that variability in irradiance within the canopy be estimated using a simple canopy extinction co-efficient model (Norman, 1982) enabling the calculation of sunlit and shaded LAI portions of the canopy. These values are then used to estimate the mean canopy relative stomatal conductance as a function of irradiance ($F_{light}$) (using the $f_{light}$ functions) according to the proportions of sunlit and shaded leaf area.

However, coniferous forest species have rather complex canopies due to the presence of needles of different ages within the canopy that will have different maximum $g_s$ values. In addition, the proportion of needles of different ages will vary over the course of the year according to the phenological stage of the tree.

To accommodate this, the deposition model divides the canopy LAI into two needle classes a) current needles and b) older needles. The variation over the course of the year in the respective ratio of these two classes is modelled according to data provided by Beadle et al. (1982) and the start of the growing season (SGS) as shown in equation [3.1.2].

$$Pc_{month} = (Pc\_max - Pc\_min)*((month - SGS_{month})/5) + Pc\_min \quad [3.1.2]$$

When $SGS_{month} \leq month \leq SGS_{month}+5$

where $Pc_{month}$ is the canopy ratio of current to older needles for that specific month (1-12); Pc_max is the maximum canopy ratio of current to older needles; Pc_min is the minimum canopy ratio of current to older needles; $SGS_{month}$ is the month (1 to 12) in which the start of the growing season occurs. Pc_max and Pc_min are given values of 0.5 and 0.1 respectively after Beadle et al. (1982). Outside the growing season $g_{phen}$ for both current and older needles is assumed to be equal to $g_{min}$.

The stomatal conductance of current year needles ($f_{phen}$) is influenced by age and modelled as described in equation [3.1.3].

$$f_{phen} = (1\text{-fphen\_a})*((yd\text{-}SGS)/fphen\_b) + fphen\_a \qquad [3.1.3]$$

when $SGS \leq yd < (SGS+fphen\_b)$

$f_{phen} = 1$

when $(SGS + fphen\_b) \leq yd \leq (EGS\text{-}fphen\_c)$

$f_{phen} = (1\text{-fphen\_a})*((EGS\text{-}yd)/fphen\_c)+fphen\_a$

when $(EGS\text{-}fphen\_c) < yd \leq EGS$

Where fphen_a = 0.2; fphen_b = 60 and fphen_c = 60.

The stomatal conductance of older needles ($f_{phen\ old}$) is assumed constant at 0.5 relative g. The phenological variation in canopy stomatal conductance ($F_{phen}$) is calculated according to equation [3.1.4]

$$F_{phen} = Pc * f_{phen} + (1\text{-}Pc) * f_{phen\ old} \qquad [3.1.4]$$

The $F_{phen}$ and $F_{light}$ values can then be substituted for $f_{phen}$ and $f_{light}$ in the overall $g_{sto}$ model equation to provide estimates of canopy stomatal conductance ($G_{sto}$) rather then needle stomatal conductance ($g_{sto}$).

The functions described above necessitate the estimation of the start and end of the growing season. For coniferous forests this could be achieved using vegetation type specific effective temperature sum models. The model for coniferous temperate trees is provided by Smith (pers. comm.) and follows equation [3.1.5].

$$ETS = \sum_{i=1}^{365} T_i - T_b \quad \text{for } T_i > T_b$$

$$ETS = 0 \quad \text{for } T_i \leq Tb \qquad [3.1.5]$$

where $T_i$ is the mean daily temperature and $T_b$ a pre-defined threshold value (5°C). The critical effective temperature sum (ETS) for budburst is 120 day degrees above $T_b$. The end of growing season (EGS) is assumed to occur when the mean daily temperature falls below 5°C.

The use of such effective temperature sum models will enable the variability in growing seasons to be mapped across Europe, this information can also be used to more accurately estimate the change in LAI, the proportion of new canopy leaves within the canopy, and the variation in potential $g_s$ ($g_{phen}$) in relation to temperature determined phenology.

The $F_{phen}$ method was broadly compared with observed $g_{sto}$ measurements made on adult Norway spruce trees at two different elevation sites in Austria (Figure 3.1.2). Throughout the growing season, when air temperature is continuously above 5 °C, the EMEP $g_{phen}$ function defines the upper limit of $g_{sto}$ reasonably well though occasionally $g_{sto}$ during August and September exceeds this potential $g_{sto}$ at both high and low elevation sites. This would suggest that the decrease in $f_{phen}$ with needle age could be made less severe to improve model predictions for these conditions. During the cold season however, the EMEP model has difficulties in predicting $f_{phen}$ because it assumes a constant minimum stomatal conductance ($f_{min}$). Measured data in Fig. 2.1.2 however, clearly show that the stomata "shut down" completely during the cold season. Thus, the model ideally, should be re-formulated to enable the cold season changes in $g_{sto}$ associated with minimum air temperature of the previous night to be incorporated.

**Figure 3.1.2**: Seasonal courses of daily mean photon flux density (PFD), air temperature (T), vapour pressure deficit (VPD), and the daily maximum stomatal conductance (Relative g) of current-year needles in the sun crown of an adult Norway spruce (*Picea abies*) tree at a low (left) and a high (right) elevation site. (Modified after Wieser et al 2000 and Häsler and Wieser unpubl.). The thin dotted lines indicate the seasonal course of the daily maximum stomatal conductance under optimum PFD, T, and VPD obtained in the field as a function of the day of the year: low altitude: y = ((-0.0000000594 ∗ x + 0.0000094) ∗ x + 0.004) ∗ x + 0.20, $r^2$ = 0.77; high altitude: y = ((0.0000000518 ∗ x – 0.0000736) ∗ x + 0.024) ∗ x –1.31, $r^2$ = 0.79. Dotted line: EMEP functions.

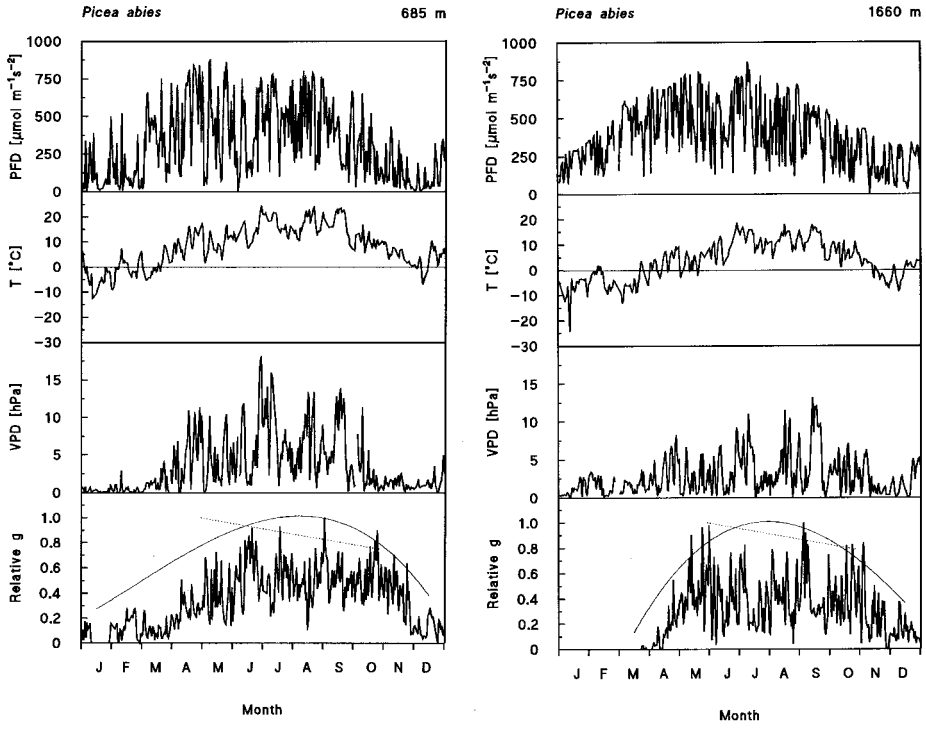


## Temperature function ($f_{temp}$)

A new $f_{temp}$ function has been introduced for the ozone deposition model. This function follows a "skewed" rather than symmetrical relationship (as has previously been used for all species and vegetation type specific relationships). As such, the EMEP formulation for $f_{temp}$ has been updated to accommodate this alternative function as described in equation [3.1.6]:-

$$f_{temp} = \max\{f_{min}, (T\text{-}T\_min) / (T\_opt - T\_min)*[(T\_max\text{-}T) / (T\_max\text{-}T\_opt)]^{bt}\}$$

$$\text{where } bt = (T\_max\text{-}T\_opt)/(T\_opt\text{-}T\_min) \qquad [3.1.6]$$

where T is the air temperature in $^{o}$C, T_min, T_opt and T_max represent the minimum, optimum and maximum temperatures for stomatal conductance. This function was primarily introduced based on the collection of additional gs data for coniferous forest trees, namely spruce (given in Jarvis et al. 1976) that suggested the Norway spruce $f_{temp}$ relationship was asymmetrical as shown in Figure 3.1.3.

Figure 3.1.3 Revised $f_{temp}$ function for Norway spruce (*Picea abies*).

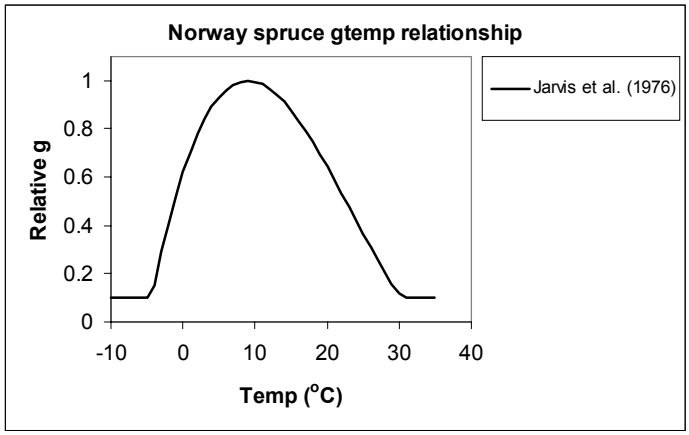


$f_{light}$

The suggested modifications to this function that would a) allow for night-time stomatal uptake to be modelled for species and; b) were found to improve model performance for Californian vineyard site are described earlier in this report in section 2.3.

*Summary*

Over the next three years a new EMEP Note will be prepared giving full details of the revised EMEP deposition model. The preparation of this Note will consider the above recommendations/suggestions for alterations to be made to the existing code. Further evaluation of alternative model formulations against observed datasets will be crucial in establishing a robust model that includes detail relevant to biological modelling yet is still appropriate for modelling at the regional scale. To this end, it may well soon be necessary to develop models suitable for application at a range of spatial scales. However, these models should be built on commonalities associated with the EMEP deposition model to ensure that flux and deposition estimates made at different spatial scales can be compared at least in semi-quantitative terms.

## 3.2 Revision of ozone stomatal flux model parameterisation

Ensuring that the stomatal flux model parameterisation is as robust as possible has been an important component of the work over the past few years, for two main reasons. Firstly, the revision of the Mapping Manual necessitated that parameterisations for wheat and potato be updated and approved through peer review by key air pollution effects scientists within the European community. This work has been written up in earlier Defra reports, and is summarised in the UN/ECE Mapping Manual (http://www.oekodata.com/icpmapping/html/manual/html), and hence will not be repeated here. Secondly, it was imperative that the most up to date and robust parameterisations were identified prior to the EMEP model runs which provide outputs to IIASA for risk assessment analysis and formulation of emission abatement policies. For this latter application, work concentrated on ensuring that the parameterisation for forest trees was "as good as possible" given available data since forests represent an important sink for ozone and hence are crucial in correctly determining the mass balance for tropospheric ozone across Europe. Details of the application of these new model parameterisations are given in EMEP Status Report 1/2003 (http://www.emep/int/).

To achieve the best parameterisation for forest trees, we have been working closely with colleagues in Sweden (PerErik Karlsson at IVL) and Spain (Ben Sanchez at CIEMAT). After discussions at various UN/ECE meetings during 2002 and 2003, the parameterisations were finalised for selected key species and pooled to provide the cover-type parameterisation as shown in Tables 3.2a and 3.2b. Significant changes made to the grouped parameterisations (shaded rows) are presented in Tables 3.2a and 3.2b in bold; the original values are presented in brackets. These values differ from those previously described in the EMEP Note of 2000 (Emberson et al. 2000). Key alterations are discussed below by cover type.

### Temperate coniferous

The parameters that have changed most significantly from those described in the 2000 EMEP note are $g_{max}$, $f_{phen}$ and $f_{VPD}$. The $g_{max}$ value has been increased based on data described in Sturm et al. (1998) and Karlsson et al. (sub). The phenology function has also been modified. fphen_a for temperate coniferous trees has been reduced to 0.2 (based on data presented in Weiser & Emberson, (in press)) although there is a case to decrease this value further (to that for $f_{min}$) since the conductance during the cold winter periods that occur in many parts of Europe will likely be minimal. This needs further consideration since the ability to determine the onset of the growing season (SGS) will also have some influence of the most suitable value for this parameter. The original fphen_b & _c parameterisation has been maintained although it has been suggested to reduce these parameters from 150 to 60 days based on data presented in Weiser & Emberson (in press) and Karlsson et al (sub). The $f_{VPD}$ function has been modified to decrease the sensitivity of the stomatal closing response to drier atmospheres reflecting data collated from Falge et al. (1996); Lange et al. (1989); Wang (1996); Sturm et al. (1996) and Aranda et al. (2002). The $f_{SWP}$ function has also been altered All other parameterisations for this cover-type remain largely the same as presented previously.

### Temperate deciduous

The parameters that have changed most significantly from those described in the 2000 EMEP Note are $g_{max}$, $f_{min}$, $f_{phen}$, $f_{temp}$ and $f_{VPD}$. The $g_{max}$ value has been revised downwards on the basis of new data for beech (Raftoyannis & Radoglou, 2002; Heath, 1998). Only beech data are used to parameterise $g_{max}$ for this cover type since the other deciduous species had significantly higher $g_{max}$ value but have a smaller coverage across Europe and hence would disproportionately affect the deposition estimates. The $f_{min}$ parameter has been reduced on the basis of lower minimum daytime $g_{sto}$ values presented for oak by Raftoyannis & Radoglou (2002). The phenology function has also been modified. fphen_a and fphen_b have both been increased in acknowledgment of the fact that the original functions were too sensitive in terms of increasing $g_{sto}$ with leaf age from the start of budburst and would give poor results if the estimation of SGS were not accurate. The temperature minimum of the $f_{temp}$ function has been reduced to accommodate the $g_{sto}$ at lower temperature value observed in northern parts of Europe (Karlsson et al., sub).

### Mediterranean Needle

The parameters that have changed most significantly from those described in the 2000 EMEP Note are $f_{min}$, $f_{phen}$ and $f_{temp}$. These changes have largely been made in accordance with the parameterisations for Mediterranean broadleaf forests for which a more robust dataset exists and hence which is considered more appropriate for model parameterisation.

### Mediterranean Broadleaf

The parameters that have changed most significantly from those described in the 2000 EMEP note are $f_{min}$, $f_{phen}$ and $f_{VPD}$. The $f_{min}$ value has been reduced in accordance with data available from Tognetti (1998) describing minimum $g_{sto}$ for *Quercus ilex*. The phenology function has been re-drawn from Caldwell et al. (1986) after consultation with Mediterranean colleagues. Finally, the $f_{VPD}$ function has been modified to decrease the sensitivity of the stomatal closing response to drier atmospheres reflecting data collated from Tognetti et al. (1998) and Elvira et al. (in press).

**Table 3.2a** Revised forest tree parameterisation. Species-specific parameters for $g_{max}$, $g_{min}$, $g_{age}$, $g_{light}$ and $g_{temp}$. A/H describes whether stomata are found over entire leaf (A=amphistomatous) or one side (H=hypostomatous).

| | $g_{max}$ | A/H | $f_{min}$ | $f_{phen}$ | | | $f_{light}$ | $f_{temp}$ | | |
|---|---|---|---|---|---|---|---|---|---|---|
| | mmol $O_3$ $m^{-2}$ $s^{-1}$ Projected | | | fphen_a | fphen_b | fphen_c | $\alpha$ | T_min | T_opt | T_max |
| | | | frac. | frac. | days | days | | °C | °C | °C |
| **Temperate Coniferous** | **160** (146) | **-** | 0.1 | **0.2** (0.5) | **130** | **130** | 0.0083 | 1 | 18 | 36 |
| *Picea abies* | 130 | - | 0.1 | 0.2 | 60 | 60 | 0.01 | -5 | 9 | 35 |
| *Pinus sylvestris* | 182 | - | 0.1 | Norway spruce | | | 0.006 | 1 | 19 | 36 |
| **Temperate Deciduous** | **134** (141) | **H** | **0.13** (0.16) | **0.3** (0) | **50** (16) | **50** (75) | 0.006 | **6** (12) | 20 | 34 |
| *Fagus sylvatica* | 134 | H | 0.1 | 0.2 | 50 | 65 | 0.006 | 0 | 20 | 35 |
| *Betula pendula* | 178 | H | 0.1 | 0.2 | 15 | 60 | 0.02 | 10 | 22 | 34 |
| Oak | 200 | H | 0.06 | 0.2 | 50 | 100 | 0.003 | Birch | Birch | Birch |
| *Quercus petraea* | 200 | H | 0.06 | 0.2 | 50 | 100 | 0.003 | Birch | Birch | Birch |
| *Quercus robur* | 210 | H | 0.06 | 0.2 | 50 | 100 | 0.003 | Birch | Birch | Birch |
| **Mediterranean Needle** | 180 | **-** | 0.13 | **0.3** (0.2) | **110** (130) | **150** (130) | 0.013 | 4 | 20 | 37 |
| *Pinus halepensis* | 122 | - | 0.1 | *Quercus coccifera* | | | *P. pinaster* | Mediterranean broadleaf | | |
| *Pinus pinaster* | 174 | - | 0.1 | *Quercus coccifera* | | | 0.013 | Mediterranean broadleaf | | |
| *Abies* species | 260 | - | 0.1 | *Quercus coccifera* | | | *P. pinaster* | Mediterranean broadleaf | | |
| **Mediterranean Evergreen Broadleaf** | **200** (213) | **A** | **0.03** (0.13) | **0.3** (0.2) | **110** (130) | **150** (130) | 0.009 | 4 | 20 | 37 |
| *Quercus ilex* | 240 | A | 0.03 | *Quercus coccifera* | | | 0.009 | 5 | 28 | 37 |
| *Quercus suber* | 200 | A | 0.03 | *Quercus coccifera* | | | 0.009 | 5 | 28 | 37 |
| *Quercus coccifera* | 180 | A | 0.03 | 0.3 | 110 | 150 | 0.009 | 5 | 28 | 37 |

**Table 3.2b** Revised forest tree parameterisation. Species-specific parameters for $f_{VPD}$ and $f_{SWP}$.

| | $f_{VPD}$ | | $f_{SWP}$ | |
|---|---|---|---|---|
| | $VDP_{min}$ | $VDP_{max}$ | $SWP_{max}$ | $SWp_{min}$ |
| | kPa | kPa | MPa | MPa |
| **Temperate coniferous** | 0.6 | **3.3** (3) | -0.76 | -1.2 |
| *Picea abies* | 0.6 | 3.8 | -0.66 | -0.98 |
| *Pinus sylvestris* | 0.6 | 2.8 | -0.7 | -1.5 |
| **Temperate deciduous** | 0.93 | 3.4 | -0.55 | -1.3 |
| *Fagus sylvatica* | 1.1 | 3.4 | -1 | -1.9 |
| *Betula pendula* | 1 | 6.8 | -0.2 | -0.5 |
| *Quercus petraea* | 0.6 | 4.7 | -0.5 | -1.2 |
| *Quercus robur* | 0.6 | 4.7 | -0.5 | -1.2 |
| **Mediterranean needle** | 0.4 | 1.6 | -0.4 | -1.0 |
| *Pinus halepensis* | 0.4 | 1.6 | *P. pinaster* | |
| *Pinus pinaster* | 0.4 | 1.6 | -0.4 | -1 |
| *Abies* species | 0.4 | 1.6 | *P. pinaster* | |
| **Mediterranean Broadleaf** | **1.8** (1.1) | **2.8** (3.2) | -1.1 | -2.8 |
| *Quercus ilex* | 1.5 | 2.8 | -0.9 | -2.8 |
| *Quercus suber* | 1.5 | 2.8 | -0.9 | -2.8 |
| *Quercus coccifera* | 1.5 | 2.8 | -0.9 | -2.8 |

# 4. Development of land-cover database

## 4.1. Summary of land cover mapping project work

This summary of the work performed to update and improve the SEI land cover map: (i) indicates the key improvements that have been made to the SEI land cover map over the past three years; (ii) briefly summarises the key attributes of the SEI land cover map for pollutant deposition and effects modelling and mapping in relation to other pan European datasets and (iii) suggests ways in which this land cover database can be optimally used within the community to facilitate deposition and effects modelling and mapping, in particular in relation to ground level ozone. A more detailed description of the new land cover database is provided in Annexe 3 of this Report and by Cinderby (2002).

### Description of the updated SEI land cover map

The SEI land cover map was originally developed in 1994 explicitly for use in modelling of the impacts of various air pollutants (specifically ozone and nitrogen) at a continental scale. As such it differs from both the CORINE and PELCOM data in that it attempts to identify an ecologically meaningful cover type and/or the dominant species across Europe. The SEI dataset has recently been heavily revised, updated and extended.

The mapping methodology employed utilises existing spatial datasets and combines them to enhance the level of information available to classify locations to a level of detail suitable for Level II ozone impact modelling. The datasets utilised in the 2002 update of the SEI land cover map are described in Table 4.1.1 The approximate scale of the combined datasets is 1:2,500,000 (approximate resolution of 2.5 $km^2$) although this varies across the map and by cover type to a minimum of 1:4,000,000.

The map contains classifications of forest type and dominant species; grassland and semi-natural vegetation types; agricultural production including crop distribution; and irrigation intensity by crop type. In addition information on soil pH patterns and rainfall have been used to further disaggregate the grassland classification. In total, the map contains approximately 450 classes of dominant species or cover type. The SEI land cover map extends across Europe to the Ural mountains and down to Turkey in order to cover the majority of the EMEP grid region.

A full description of the updated version of the SEI land-cover map was presented at the UN/ECE Ad Hoc Expert Panel meeting held in Harrogate, U.K. in June 2002. The paper presented at this meeting can be downloaded at (http://www.york.ac.uk/inst/sei/APS/projects.html).

Table 4.1.1 Datasets utilised in the revision of the SEI land cover map.

| Data Set | Source | Scale/Resolution | Date of Preparation |
|---|---|---|---|
| Land Use Map of Europe | Food and Agriculture Organisation | 1:2,500,000 | 1980 |
| Remote Sensing Forest Map of Europe | European Space Agency | 1:2,000,000 | 1992 |
| Global Land Cover | International Geosphere-Biosphere Project | 1km by 1km | 1999 |
| Forests of the USSR | World Conservation Monitoring Centre | 1:2,500,000 | - |
| Land Use of the Former USSR | GUGK | 1:4,000,000 | 1991 |
| Land Cover | Pelcom | 1.1km | 2000 |
| Soil Map of the World | Food and Agriculture Organisation | 1:5,000,000 | 1981 |
| Coastline | Bartholomew's | | |
| Global Land Cover | International Geosphere-Biosphere Project | 1km by 1km | 1999 |
| Agrostat Crop Database | Food and Agriculture Organisation | | 1999 |
| NUTS Level II Eurostat Crop Database | Eurostat | | 1999 |
| Map of Global Irrigation | Doll and Siebert | $0.5^{o}$ by $0.5^{o}$ | 1999 |
| Soil Map of the World | Food and Agriculture Organisation | 1:5,000,000 | 1981 |
| Soil Map of the European Union | Corine | 1:1,000,000 | 1984 |
| Annual Average Amount of Precipitation, Asia | World Meteorological Organisation | 1:10,000,000 | 1981 |
| Annual Average Amount of Precipitation, Europe | World Meteorological Organisation | 1:5,000,000 | 1970 |
| WISE Soil Database Version 2.1 | International Soil Reference and Information Centre | | 1995 |

## Key Improvements to the SEI land cover map

The previous version of the SEI land cover map was compared to the CORINE and PELCOM data sets by the CCE (de Smet & Hettelingh (2001)) and a number of weaknesses in the original SEI map were identified. Over the past two years additional data have been incorporated with, or replaced, the original SEI map layers to address some of the criticisms of the data set identified by the CCE.

Particular improvements include:

Extent and borders: The SEI land cover maps spatial extent has been increased to include Turkey and Cyprus. In addition the identification of coastlines has been improved through the use of higher resolution data. Country borders are not included in the revised data sets as the map is intended for use at the European scale, rather than for national or sub-national activities. The extent of the revised map can be seen in Figure 4.1.1.

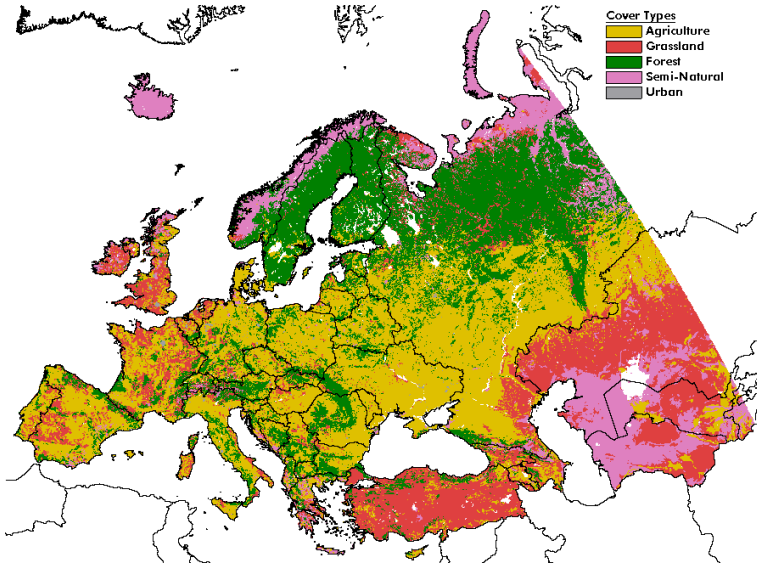


Figure 4.1.1. Extent of the revised SEI land cover map indicating the broad land cover classes

**Increased classification detail**: The level of detail in the SEI land cover classes has been increased through the inclusion of the new data layers. Seventy-five dominant forest species are now identified; grassland and semi-natural vegetation have been combined with information on soil pH and precipitation regime; and agricultural crop patterns have been classified.

**Agricultural distribution**: The spatial distribution of agricultural land has been improved through the inclusion of new datasets, in particular, the IGBP Global Land Cover (1999). These spatial datasets have been linked to agricultural crop production statistics from EUROSTAT (NUTS Level II) and FAOSTAT to identify the actual distribution of crops grown across Europe and the yields associated with them for the base year of 1999.

**Irrigation**: Gridded information on the level of irrigation across Europe has been included in the update. This information has been linked to the agricultural distribution statistics and information on irrigation management by country to produce data showing the distribution and level of irrigation by crop type across Europe.

A comparison of the revised SEI land cover map with other European data sets has been performed including CORINE and PELCOM. The comparison indicates that the SEI map has a Kappa (khat) statistic agreement with the CORINE map of 50% at the 95% confidence level. This comparison utilised all pixels and as such represents the harshest comparison that could be performed. All edge effects (where the boundary between two classes is disputed) were included in the calculation of the statistics – if point samples had been used in the calculation the Kappa value could be considerably higher.

The SEI map was made freely available to all interested parties in late summer, 2003. The layers available include all forest, grassland and semi-natural information. Dominant agriculture and irrigated crops are included. The possibility of including the detailed agricultural distributions is being investigated (in order to avoid copyright infringements). The data have been exported into Arc/INFO export format (.e00 files) and are checked for integrity. The export files are now available, free of

charge, via the SEI website for ftp download (see the SEI website for more details of availability – www.seiy.org).

### Harmonisation issues

In order to facilitate comparison of model results, investigate the impact on results of differences between spatial data sets, and ease the integration of national and continental data the possibility of harmonising land cover information for Europe to a consistent classification scheme is being investigated. EUNIS is a classification system for defining different habitat types but does not have a geographical reference itself. In combination with suitable geographical land use information it may provide the data needed for mapping critical loads and levels and their exceedance. The recent revision of the UN/ECE Mapping Manual recommends the re-classification of European land cover datasets using the EUNIS level 2 habitat classification codes. However, this level of detail may not be sufficient to enable ozone effects modelling and mapping. For example, the new concentration and flux based critical levels for ozone (suggested in the recent Mapping Manual revision) require information describing the distribution of specific agricultural crop species (i.e. wheat, potato and tomato). None of the EUNIS classification levels provide this level of detail, as such it may be necessary to use a modified version of EUNIS to allow for such situations in current and future critical level mapping.

In addition, in the future it may be necessary to classify certain semi-natural vegetation community types that research identifies as being sensitive to both ozone and nitrogen deposition. The EUNIS level 2-classification scheme would appear to provide a sufficient level of detail for this to be possible, although this may need to be reconfirmed as new information becomes available.

The possibility of harmonising land cover information to the EUNIS classification is currently being investigated by the CCE and CORINE projects. The potential for mapping EUNIS categories using a reclassification of the existing SEI categories has recently been explored. The existing SEI land cover classification can be directly translated into EUNIS Level 1 habitat classification codes – however, as stated above, these do not contain sufficient detail for the assessment of ozone sensitive species or the impacts of air pollution in general on ecosystems – the original justification for the development of the SEI map.

At the second level of the EUNIS classification, the existing SEI land cover grassland classes have been assessed in detail for their compatibility with EUNIS. The SEI grassland classes can be related to the majority of the subdivisions of the grassland and tall forb habitat (E EUNIS class). The current conversion between the EUNIS Level 2 grassland and tall forb habitat classes can be obtained from the SEI map. However, in order to reliably identify all of the subdivisions of the EUNIS level 2 and 3 classes of grassland and tall forb habitats, additional spatial data will have to be incorporated with the SEI data. In particular, information on soil moisture regimes, altitude, salt and heavy metal affected soils and potential habitat distribution will potentially be required to improve the current reclassification of the SEI land cover map into the EUNIS nomenclature.

The potential for identifying the other Level 2 classes of the EUNIS scheme with the existing SEI data vary by cover type. The SEI classification has a very good match with the woodland and forest habitats (G), agriculture and horticulture (I), and unvegetated or sparsely vegetated (H). The existing SEI classification can be translated adequately for the coastal habitats (B) and heathland, scrub and tundra (F) EUNIS level II classes. However, the existing SEI classes do not correspond well with the EUNIS level II mire, bog and fen (D), and constructed, industrial and artificial habitats (J). The poor

overlap of the SEI scheme with these areas of EUNIS classification is due to a combination of the spatial resolution of the SEI map, the focus of the SEI classes (concentrating on impacts of air pollutants on vegetation) and the level of detail in the EUNIS D class which would be very difficult to identify across Europe using the SEI mapping methodology of utilising and enhancing existing European-wide datasets.

### Conclusions

The information provided in this summary has identified the following issues for consideration by the modelling and mapping community:-

The SEI land cover map has been significantly revised and updated since the comparison of European land-cover datasets was performed by CCE (de Smet & Hettelingh, 2001) and hence the recommendations made in that paper as to which pan-European data set is most suitable for pollution deposition and effects modelling and mapping should be revised.

Application of the new critical levels for ozone suggested in the revised version of the Mapping Manual will require more detailed land cover data (i.e. species-specific rather than vegetation specific) and additional spatial information describing associated biological, economic and management practices. Such data are not readily available in many of the existing pan-European datasets.

It is unlikely that any one pan-European spatial dataset can provide all the information that might be needed for current and future critical loads/levels work. As such, the mapping and modelling community should consider using a variety of different spatial datasets appropriate to their needs. This will require that each of the datasets uses a common classification scheme (e.g. an appropriately modified version of the EUNIS level 2 scheme) and that issues surrounding the provision by EMEP of ecosystem specific deposition values be addressed to ensure consistency between European and national scale deposition and effects modelling and mapping.

In relation to the above, an important role for the SEI map should be to provide spatial data that will be freely available to users to supplement national or European land cover datasets.

## 4.2 Uncertainty in mapping of agriculture

This research was recently completed, and has not been reported either in previous Defra reports, or in other papers and reports. The aim of this work was to provide an indication of the uncertainty in ozone flux estimates related to land-cover data. One of the most difficult land cover types to define in terms of distribution is agriculture, and specifically the location of particular crop species. Given the recent revisions to the UN/ECE Mapping Manual (i.e. the inclusion of methods to estimate flux to wheat and potato) it is crucially important that the distribution, and associated yield of these two crops be mapped as accurately as possible.

The classification of agriculture in the SEI land cover database uses four spatial data sets linked to two agricultural statistical databases. The spatial databases used to identify the location and type of agricultural production across Europe were the existing SEI land cover information indicating the extent of agriculture and the distribution of various types of horticulture and the IGBP data set that contained information on the extent and type of agricultural production. These combined datasets delimited the extent of agriculture across Europe. This spatial data set was then combined with

agricultural databases indicating the type, extent and yield of agriculture in the European NUTS regions and countries. For the general agricultural class, 'Cropland', the statistics were used to determine the actual percentage of different crop types grown (excluding horticulture) in that country. For the UK a similar activity was performed for NUTS Level II regions allowing detailed identification of the distribution of crops in the UK.

The resulting distribution of wheat is shown in Figure 4.2.1.

Figure 4.2.1 Distribution of wheat in the UK

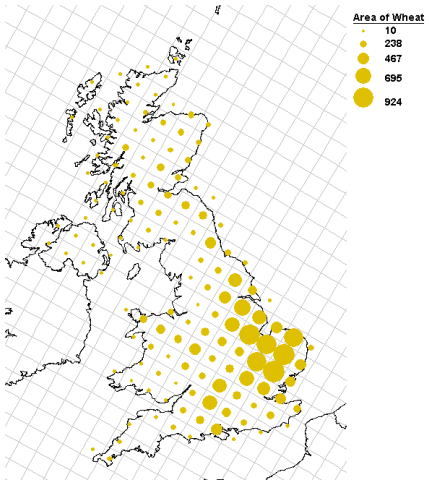


A previous Defra report described a comparison that was made between the SEI land cover dataset and the CEH Land Cover Map (LCM 2000). The level of agreement between the two maps for arable cultivation (including the set aside class of the CEH land cover map) is considered average, with 63% of the area classified as arable on the SEI map overlapping with the CEH class. Tables 4.2.1 and 4.2.2 show the levels of agreement, using varying thresholds indicating the level of overlap between the areas of classes represented on the two datasets. The thresholds are 5% (excellent), 15% (good), 25% (OK) and >25% (poor).

Table 4.2.1. Arable class comparison results. Arable cereals, arable horticulture and set aside classes from the CEH map versus the wheat and barley areas combined from the SEI map.

| Cover Type | Agreement Level | Percentage of EMEP 50km Grids | Cumulative Percentage |
|---|---|---|---|
| Arable | Excellent | 24% | 24% |
| | Good | 28% | 52% |
| | OK | 9% | 61% |
| | Poor | 39% | 100% |

Table 4.2.2. Relative percentage area of arable class on CEH and SEI maps. CEH class includes only arable cereal, arable horticulture and set aside classes.

| Map | Cumulative Percentage Area |
|---|---|
| CEH | 3667% |
| SEI | 5370% |

These statistics were used to estimate the range in wheat distribution (in terms of coverage in hectares) for each EMEP grids; the actual value being determined by the SEI map and the range around this value estimated as the percentage agreement with the CEH land cover map. This estimate was made assuming that those EMEP grid squares with the largest wheat distributions were most likely to be closest to the correct value, since larger areas are generally mapped with greater accuracy. Figure 4.2.2 shows the range, by grid square, in wheat distributions from a minimum (low) to maximum (high) coverage in relation to the "actual" distribution determined according to the SEI map.

Figure 4.2.2 The range in % coverage of wheat by grid squares.

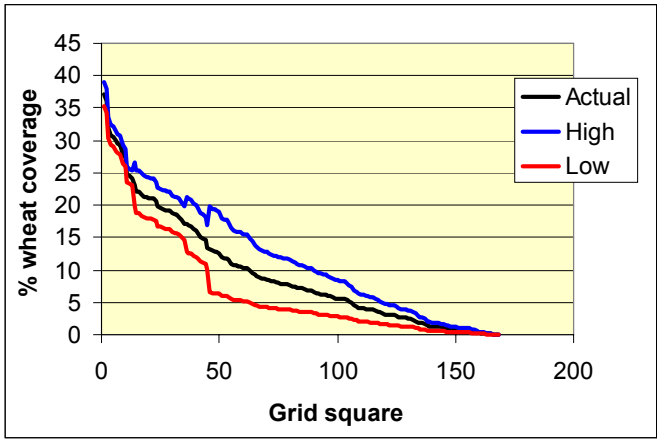


To indicate how the uncertainty associated with wheat distribution might affect ozone flux mapping it is necessary to compare the spatial distribution of the wheat uncertainty statistics with the spatial distribution in magnitude of ozone fluxes. Initially, it was intended that this work would investigate the coverage uncertainties in relation to calculated ozone deposition velocities for the UK. However, a separate piece of work, performed by an MSc student at York University, has produced a dataset describing effective stomatal ozone flux for wheat in accordance with the new methodology described in the UN/ECE Mapping Manual. The use of these data provide a much clearer indication of the importance of the range in the wheat coverage statistics since this method is designed specifically for wheat and specifically for application at the national (e.g. UK) scale.

The MSc data provided estimates of the yield reductions (as relative yield) caused by ground level ozone for the year 2000. The data describing wheat distribution as a percentage of each EMEP grid square was converted to wheat coverage in ha (since each EMEP square covers 2500 $km^2$ or 250 000 ha). Assuming that average wheat yields are approximately 8.01 tonnes per hectare (as indicated by Defra statistics) we can calculate the yields (in tonnes) associated with each grid square for the range of wheat distribution statistics (Figure 4.2.3). In addition, it is possible to assess the influence of ozone flux on the range in estimated yields associated with the wheat distribution statistics. This is shown in Figure 4.2.4 were, for each grid square, the range in yields both with and without the influence of ozone are shown.

Figure 4.2.3 The yield (in 000's tonnes) for each EMEP grid square for the range of wheat distribution statistics

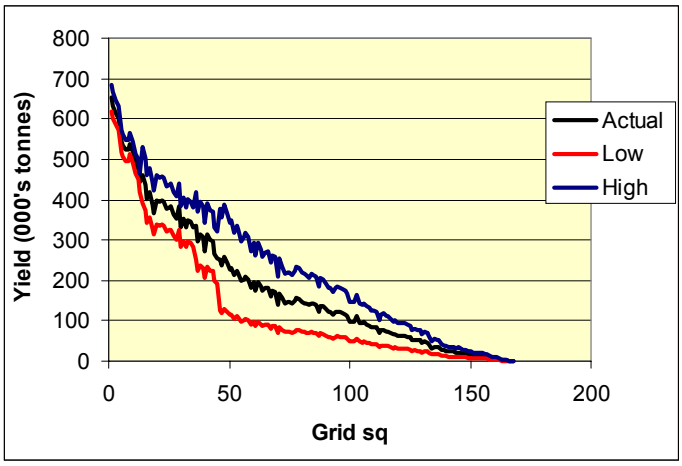


Figure 4.2.4 The range in yields (in 000's tonnes) for each EMEP grid square with and without the influence of ozone

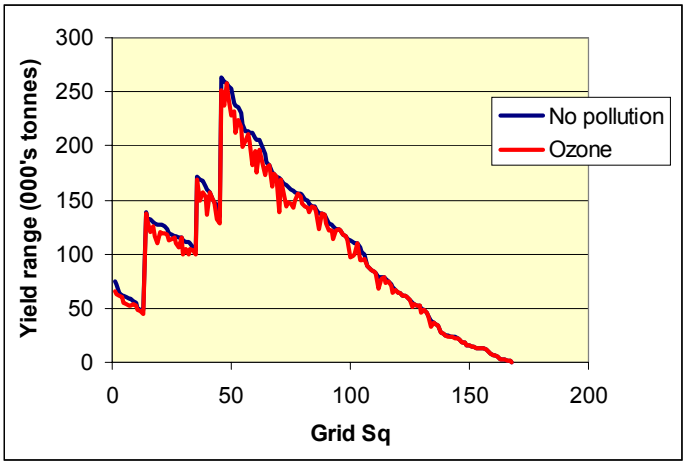


Figure 4.2.3 shows that uncertainty in the estimated yield is greatest for those grid squares which have a moderate coverage of wheat; those grid squares that have a high wheat coverage are mapped reasonably accurately whilst those grid squares with a low wheat coverage have little effect on yield (even though their mapping is considered least accurate). Figure 4.2.4 shows that the influence of ozone acts indiscriminately on all grid squares; i.e. there is no apparent bias – areas with highest uncertainty in wheat coverage are not correlated to those areas experiencing greatest ozone impact.

However, Figure 4.2.4 does show that the uncertainty in wheat distribution across the UK translates into uncertainty in respect of wheat yields, and yield reductions attributable to ozone. In terms of total UK wheat yield, the range for conditions excluding effects of ozone is between 23.4 and 41 million tonnes and for conditions allowing for ozone impacts on yield the range is between 22 and 38.7 million tonnes. It is also interesting to compare the wheat production statistics estimated from the

SEI map with the actual statistics collected for the UK. In 2000, actual wheat production was approximately 16.7 million tonnes. This difference can be attributed primarily to the over-estimation of the wheat coverage by the SEI map (assuming 4, 027 thousand ha) compared with an actual wheat coverage of 2, 086 thousand ha (Defra statistics).

This highlights the urgent need to expand efforts in the future to improve land cover mapping, both at the national and international scale. Incorporation of national statistics data with the SEI land cover database would vastly improve the mapping of crop distributions and associated yield data for Europe; this work is vitally important when assessing the economic implications of ozone impacts, the driving force behind the development of flux based approaches.

# 5 Modelling ozone detoxification

## 5.1 Introduction

The phytotoxicity of ozone arises primarily as a result of the oxidative stress it imposes on cell membranes – particularly the plasmalemma (the cell membrane inside the cell wall which serves a number of vital functions and acts as the boundary between cell and external environment). Having gained entry to the leaf interior, *via* the stomata, ozone dissolves readily in the aqueous matrix associated with the walls of mesophyll and palisade cells (i.e. the leaf apoplast). This compartment contains a variety of soluble and cell wall-bound constituents that are known to react rapidly with $O_3$ in *ex vivo* experiments – not least, ascorbate (Vitamin C). It is thus possible that a significant fraction of the environmentally-relevant flux of ozone entering leaves is scavenged (and effectively detoxified) through such reactions. Drs. Barnes and Plöchl *et al*. have modelled the diffusion-reaction network (on the assumption that ozone reacts directly and solely with cell wall-localised ascorbate) following ozone uptake into the leaf interior (Plöchl *et al*. 2000). Their PC-based model (SODA: Simulated Ozone Detoxification in the Leaf Apoplast see Appendix 5.1) allows, for the first time, the simulation of the defensive capability afforded by the leaf apoplast (based on the direction reaction of ozone with cell wall-localised ascorbate). Although limited by the boundaries of current knowledge, SODA provides an opportunity to estimate ozone flux to the plasmalemma – a parameter governing flux thresholds for damage and more closely related to impacts on vegetation than cumulative ozone exposure (AOT40) or stomatal ozone flux.

The work under this work package had three major aims:-

1. Provision of additional data underpinning the role of cell wall-localised ascorbate in ozone detoxification
2. Undertaking of required field-based measurements to allow diel simulations of ozone flux via SODA for spring wheat and NC-S clover
3. Exploration, with UoB and SEIY, with Dr. Plöchl (ATB-Potsdam), of a framework to extend current stomatal flux models to facilitate the estimation of ozone flux to the plasmalemma.

Defra funds were used to partially support a research student (Ms. Holly Smith) to undertake some of the key measurements required. Added value has been provided through (i) supplemental funding provided by Newcastle University (to create a 3-year research studentship), (ii) the allocation of Marie Curie PhD support funds to enable training of Spanish student funded by Spanish Ministry grant to conduct measurement campaign on field-grown wheat in Spain, (iii) utilisation of transgenic plants created during industrially-funded contracts and (iv) the allocation of a NERC-CASE funded PhD student to undertaking the designated work on NC-S clover. Dr Ben Gimeno (CIEMAT, Spain) also contributed significantly to this work.

## 5.2 Role of cell wall-localised ascorbate

(i) Maddison *et al*. (2002). *Planta* 214: 383-391. Leaf L-ascorbate content was increased two-fold by feeding hydroponically-cultivated plants L-galactono-1,4-lactone (GAL) (an immediate precuror of ascorbate biosynthesis). Plants were grown in controlled environment chambers ventilated with charcoal/Purafil® filtered air (CFA), and administered one of two $O_3$ fumigation regimes; chronic exposure (75 nmol $O_3$ $mol^{-1}$ for 7 h $d^{-1}$ for 21 d) and acute exposure (180 nmol $O_3$ $mol^{-1}$ for 9 h). Chronic $O_3$ exposure decreased root growth by 11% in plants maintained in pure nutrient solution (-GAL), but resulted in no change in root growth in GAL-fed plants (+GAL). Similarly, GAL-feeding counteracted the negative effects of $O_3$ on $CO_2$ assimilation rate observed in control plants (–GAL). Under acute $O_3$ exposure, GAL-fed plants showed no visible symptoms of injury, which were extensive in plants not fed GAL. Leaf $CO_2$ assimilation rate was decreased by acute $O_3$ exposure in both GAL treatments, but the extent of the decline was less marked in GAL-fed plants. No significant changes in stomatal conductance resulted from GAL treatment, so $O_3$ uptake into leaves was equivalent in +GAL and -GAL plants. Feeding GAL, on the other hand, enhanced the level of ascorbate, and resulted in the maintenance of the redox state of ascorbate under acute $O_3$ fumigation, in both the leaf apoplast and symplast. The effect of GAL-treatment on ascorbate pools was consistent with the reduction in $O_3$ damage observed in GAL-fed plants. Attempts to model $O_3$ interception by the ascorbate pool in the leaf apoplast suggested a greater capacity for $O_3$ detoxification in GAL-fed plants, which corresponded with the increase in $O_3$ tolerance observed. Data revealed strong evidence to support a role for cell wall-localized ascorbate in ozone detoxification, but highlighted a need for a better understanding of the role played by additional constituents of the leaf apoplast in the attenuation of environmentally-relevant $O_3$ fluxes.

(ii) Sanmartin *et al*. (2003) *Planta* 216: 918-928. Transgenic tobacco (*Nicotiana tabacum* L. var. Xanthi) plants over-expressing cucumber ascorbate oxidase (CAO) were used to examine the role, and sub-cellular localization, of ascorbate in mediating tolerance to ozone. Three homozygous transgenic lines, chosen on the basis of a preliminary screen of AO activity in the leaves of 29 lines, revealed up to a 380-fold increase in AO activity, with expression predominantly associated with leaf cell walls. Over-expression of AO resulted in no change in the total ascorbate content recovered in apoplast washing fluid (AWF), but the redox state of ascorbate was reduced from 30% in wild type leaves to below the threshold for detection in CAO over-expressing plants. Levels of ascorbate and glutathione in the symplast were not changed in CAO over-expressing plants, but the redox state of ascorbate was slightly reduced, while that of glutathione was slightly increased. Transgenic plants exposed to chronic ozone stress (100 nmol $mol^{-1}$ for 7 h $d^{-1}$) exhibited a marked increase in visible foliar injury (see Figure 5.1), and a greater pollutant-induced reduction in both the light-saturated rate of $CO_2$ assimilation ($A_{350}$) and the maximum *in vivo* rate of Rubisco carboxylation ($V_{cmax}$) in comparison with wild type plants. Transgenic plants also exhibited a more-pronounced decrease in $CO_2$ assimilation rate when exposed to an acute level of ozone (300 nmol $mol^{-1}$ for 8 h). Stomatal conductance, hence $O_3$ uptake, was unaffected by CAO over-expression. The data lend strong support to a role for cell wall-localised ascorbate content/redox status in mediating ozone tolerance (i.e. defence against ozone).

**Figure 5.1.** Impacts of apoplast ascorbate manipulation (using transgenic expression of CAO in cell wall) on ozone-induced visible leaf injury.

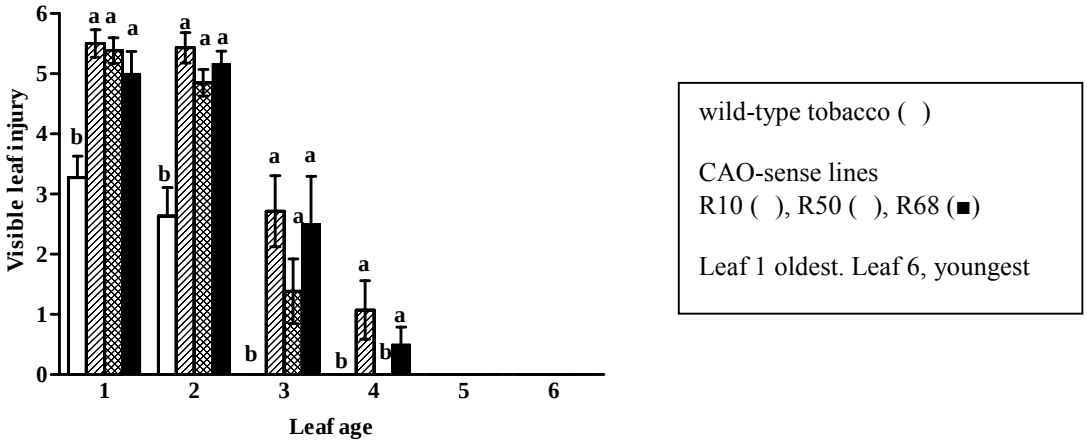


(iii) Pignocchi *et al.* 2003a,b; Smith H, Foyer CH, Barnes JD (in preparation). Sense and antisense technologies were employed to manipulate ascorbate oxidase (AO) activity in the apoplast of tobacco (*Nicotiana tabacum* L. var. Petit Havana, mutant SR1). Manipulation of AO activity resulted in no significant change in whole leaf ascorbate (AA) content or stomatal conductance, but dramatically affected apoplast ascorbate content/redox status. Through the transgenic enhancement of AO activity, the redox state (AA / AA plus oxidised ascorbate x 100) of ascorbate in the leaf apoplast was markedly reduced, while the suppression of AO activity increased it. In comparison with WT plants, lines over-expressing AO exhibited a marked increase in visible foliar injury, while antisense plants exhibited reduced visible injury, when exposed to acute ozone stress (300 nmol $mol^{-1}$ for 36 h) (see Figure 5.2). Moreover, sense lines exhibited a greater pollutant-induced reduction in both the light-saturated rate of $CO_2$ assimilation ($A_{350}$) and the maximum *in vivo* rate of Rubisco carboxylation ($V_{cmax}$), while antisense lines exhibited less response to $O_3$ than WT plants.

**Figure 5.2.** Impacts of apoplast ascorbate manipulation (using sense ($AO_{ox}$) and antisense ($AO_{KO}$) manipulation of AO in cell wall) on ozone-induced visible leaf injury.

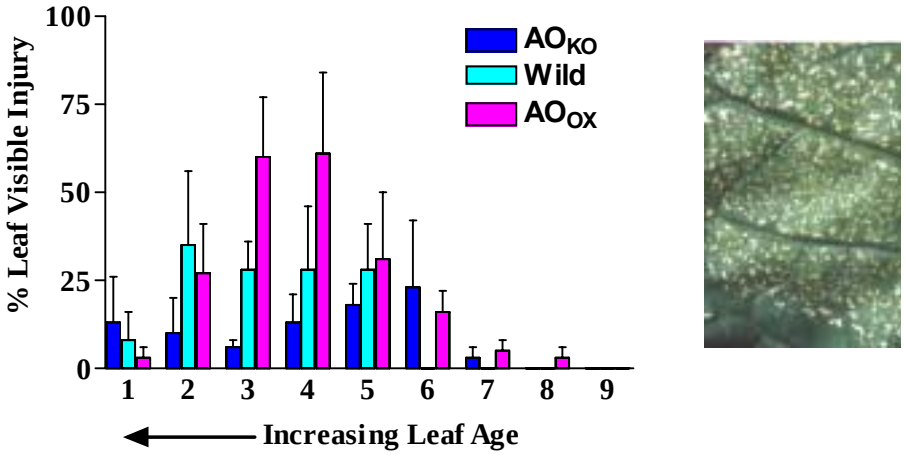

A strong positive relationship ($r^2$ =0.756) existed between AO expression and plant height (and accumulated biomass/plant growth rate); sense plants were taller than the WT (i.e. enhanced AO activity promoted growth) while anti-sense plants were shorter (i.e. decreased AO activity reduced growth). The data lend further support to a role for cell wall-localised ascorbate content/redox status in mediating ozone tolerance (i.e. defence against ozone) and suggest that $O_3$-induced shifts in apoplast ascorbate content/redox status maybe linked to suppressions in plant growth in a more-fundamental manner than previously considered.

### Future needs

Further work is required to improve our understanding of the role of apoplast ascorbate content/redox state in governing the reaction of vegetation to ozone. In particular studies need to address:

- The role of apoplast ascorbate content/redox state in controlling/signalling the upregulation of cellular defences to combat ozone-induced oxidative stress, since it is possible that shifts in apoplast ascorbate content/redox status exert pleiotrophic effects over-and-above those associated with the role of apoplast ascorbate in the direct scavenging of ozone i.e. measurements of apoplast ascorbate content/redox state may act as a surrogate for other oxidative defences,
- The relationship between $O_3$-mediated shifts in apoplast ascorbate content/redox state and impacts on plant growth

## 5.3 Field measurements for wheat and clover

(i) J. Cardoso-Vilhena, H. Smith & D. Bass-Pickin (unpublished). A reliable method for the isolation of uncontaminated apoplast fluid (AWF) from the flag leaf of field-grown spring wheat, and the analysis of whole leaf ascorbate content/redox state, was successfully developed. Despite more than three months of intensive effort it proved impossible to reciprocate this success with field-grown NC-S clover. Successful extractions of AWF could be accomplished repeatedly with laboratory-grown material, but with field-grown clover it proved impossible to effectively prevent the oxidation of ascorbate during the isolation of apoplast washing fluid (despite employment of a range of infiltration buffers, buffer formulae plus the incorporation of various enzyme inhibitors). Nevertheless a substantive stomatal conductance database was collected for open-top chamber-grown NC-S clover and this, along with associated micro-meteorological data, will be transferred to ICP Vegetation database to assist in the development of flux modelling approaches for clover. As a consequence of the problems, subsequent studies focussed on wheat, but experiments were extended to so as to facilitate the duplication of field-based investigations in the UK and Spain and create a robust database upon which to ultimately base the derivation of an algorithm describing the way in which SODA-computed $M_{res}$ is influenced by environmental variables (see section 5.4).

(ii) H. Smith (unpublished). Ultra-thin sections of field-grown flag leaves of spring wheat were prepared for electron microscopy at different times of the day and at contrasting stages of

development. EM-derived measurements on multiple sections were used to parameterize SODA with the required anatomical data for the flag leaf of wheat (see Appendix 5.2).

(iii) H. Smith & D. de la Torre (unpublished). Diel measurements of flag leaf apoplast/sympast ascorbate content were made independently mid-season (respectively) at multiple development stages. Wheat flag leaves were sampled at two experimental field sites: in the UK (Triticum aestivum L. cv. Hanno; Close House Experimental Station, Heddon-on-the-Wall, Northumberland) and in Spain (Triticum durum Desf. cv. Camacho; El Encin, IMIA , Madrid). In addition, on site monitoring equipment (with back-up) logged environmental variables (ozone concentrations, PPFD, temperature, RH, VPD) and stomatal conductance of flag leaves was tracked over the leaf lifespan to create a substantial independent database (>4000 measurements) to be used downstream for the validation of multiplicative stomatal flux models derived from Swedish data for Scandinavian genotypes of wheat (submitted to DEFRA within recent 'umbrella' project led by Dr. G. Mills). Data were collected over two consecutive years in order to fully-validate findings. The diel marches presented (Figure 5.3), represent data collections for individual years (2002 for UK) and 2003 (for Spain). The datasets showed remarkable consistency considering the independent manner in which the data were collected. Whilst there was no significant diel differences in measured anatomical features (see Appendix 5.1), the ascorbate content of the leaf apoplast exhibited a maximum during the day and attained a minimum at night-time (driven to some extent by light: [apoplast ascorbate] = 0.019PPFD +22.32 $r^2$ = 0.23 P< 0.0001; Temperature: [apoplast ascorbate] = 1.81temp –0.986 $r^2$= 0.14 P< 0.0001; VPD: [apoplast ascorbate] = 11.01VPD + 14.81 $r^2$= 0.1 P< 0.0001; Figure 3). Interestingly, (i) the attainment of the highest levels of apoplast ascorbate appeared to be out of synchrony in UK/Spanish datasets: levels attaining a maximum between 10.00 and 13.00 in the UK studies and between 14.00 and 16.00 in the Spanish studies.

**Figure 5.3**. Diel shifts in apoplast/symplast ascorbate content of the flag leaf of spring wheat. Measurements were made on *Triticum aestivum* L. cv. Hanno at a site in the UK and on *Triticum durum* Desf. cv. Camacho at a site in Spain.

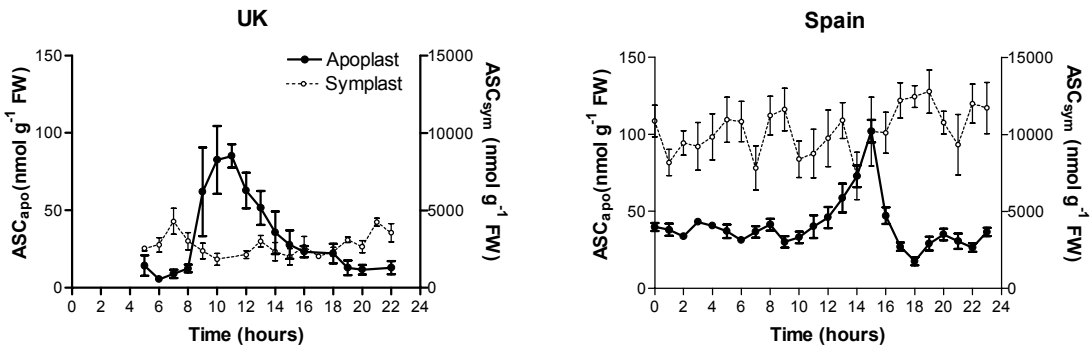


(ii) apoplast ascorbate levels were high for only a part of the day, the computed ozone flux to the plasmalemma (derived using SODA employing measurements of stomatal conductance and anatomical features plus 3-year average hourly ozone data for the respective sites) varied significantly during the day such that computed ozone detoxification potential/neutralisation capacity varied from c. 50% of the potential (i.e. $g_{s(max)}$) ozone flux to <10% early and late in the day (Figure 5.4).

**Figure 5.4**. Computed ozone flux to the plasmalemma based-on measured anatomical data, ascorbate levels and stomatal conductance – employing 5-year hourly average ozone data for month of collection (May) at site in Madrid, Spain (attaining midday max 45 ppb) and actual daily ozone data for UK site in NE England (attaining a midday max of c. 50 ppb).

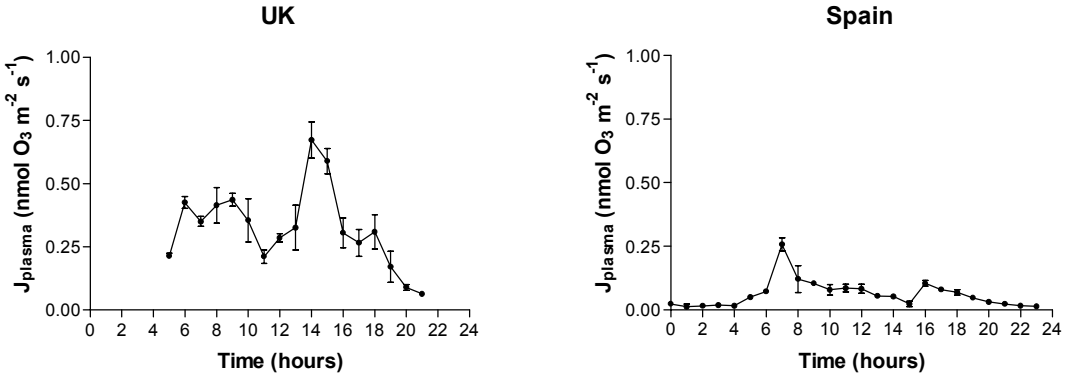


These data illustrate (i) the threat posed by lower levels to vegetation under UK conditions versus those in Spain (with $g_s$ taken into account) and (ii) potential need to weight hourly ozone concentrations/fluxes, since relatively high ozone fluxes at night (in plants that show incomplete stomatal closure and/or localities where $O_3$ concentrations commonly remain high at night e.g. uplands and the Mediterranean), early morning and late afternoon are likely to be particularly damaging (i.e. critical flux thresholds may differ over the course of the day). Data also revealed that diel shifts in apoplast ascorbate levels were not mirrored in the symplast, though levels were notably higher under Spanish conditions – possibly reflecting the greater need of chloroplasts under Mediterranean conditions to protect themselves against light-induced oxidative stress.

## 5.4. Methods of Modelling

(i) Linkages. Examination of ways to formally link the existing Emberson/Ashmore/Pleijel stomatal flux model with the Plöchl/Barnes apoplast detoxification model indicated that the combination of the two models was not the most effective or feasible option, at this stage. An approach was developed to allow the detoxification processes simulated by the Plöchl/Barnes model to be incorporated into modelling/mapping approaches through the incorporation of an additional (discrete) resistance term ($M_{res}$): representing the resistance afforded by the diffusion-reaction network between intercellular spaces and the plasmalemma. SODA was translated and recoded, and a new iterative version of the model produced by Dr. Plöchl, allowing multiple simulations (over a range of stomatal conductances, ozone concentrations and apoplast ascorbate concentrations) to be conducted in single runs of the model. In addition, new model output parameters were calculated incl. ozone flux to the plasmalemma, stomatal ozone flux and a summative resistance parameter: mesophyll resistance (still under development). One potentially important feature of model output from the Plöchl/Barnes model has been the illustration that the intercellular ozone concentration is close to, but not actually zero – as is commonly assumed. Calculations indicate finite intercellular concentrations of ozone, as illustrated in Figure 5.5.

**Figure 5.5**. Computed intercellular ozone concentrations over a range of environmentally-relevant conditions

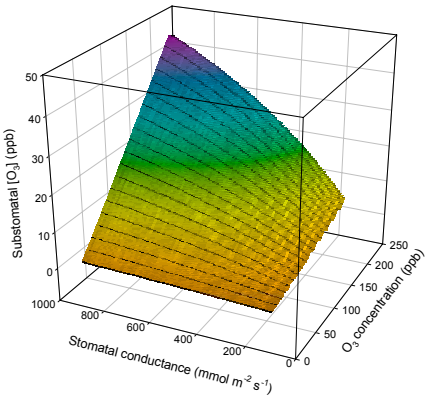


(ii) Consistency of SODA output with empirically-derived critical flux thresholds. The best correlations between stomatal uptake of ozone and relative yield are obtained using an ozone uptake threshold (applied using a constant flux value removed hour-by-hour from the calculated stomatal uptake of ozone per unit sunlit leaf area). At maximum stomatal conductance the empirically-derived threshold currently employed for assessing the impacts of ozone on the yield of spring wheat and potato is 6 nmol $O_3$ $m^{-2}$ $s^{-1}$ (which corresponds to a concentration threshold of c. 20 nmol $mol^{-1}$). This is close to the background level of ozone in the troposphere (i.e. the level existing in the pre-industrial era) and corresponds well with the midday flux threshold (c. 5 nmol $O_3$ $m^{-2}$ $s^{-1}$) derived for the flag leaf of wheat employing our extracellular detoxification model parameterized using data collected during the course of the present study (Figure 5.6).

**Figure 5.6**. Mid-day critical flux threshold derived for wheat flag leaf using fully-parameterized Plöchl/Barnes extracellular detoxification model.

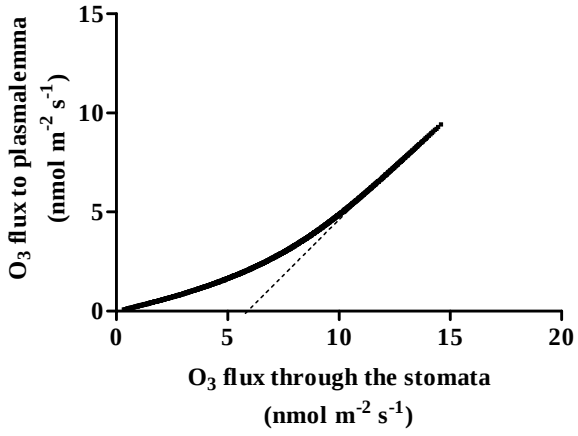

(iii) Development of a simple algorithm describing the manner in which environmental and developmental factors drive shifts in detoxification (i.e. neutralisation) capacity. The data required to deliver this algorithm for spring wheat have been collected within the framework of the current project. Figure 5.6 shows part of the database available that could be used to compute a multiplicative algorithm (using boundary line analysis) describing shifts in mesophyll resistance ($M_{res}$) (to be calculated by Plöchl/Barnes based on current understanding of ozone diffusion-reaction following uptake into the interior of the flag leaf of wheat) induced by key environmental and developmental drivers.

### Future needs

(i) Derivation of a multiplicative model from data collected from field-grown plants (see Figure 5.7), describing shifts in diffusion-reaction following ozone uptake in relation with the timing of ozone peaks during the day and environmentally-induced/phenologically-related shifts in neutralisation capacity. Employing the same approach adopted for the derivation of multiplicative stomatal flux models (Emberson et al. 2000), we will utilise the boundary line technique to derive an algorithm simulating shifts in ozone neutralisation capacity (i.e. flux threshold) based on the manner in which maximum daytime mesophyll resistance ($M_{res(max)}$; computed for wheat flag leaves using Plöchl/Barnes detoxification model) is driven by key variables (light [PPFD], temperature (temp), ozone, leaf phenology (phen), time of day (time) and soil moisture availability (SMA)).

i.e.:

$$M_{res} = M_{res(max)} * (\min(M_{res(phen)}, M_{res(ozone)}) * M_{res(SWA)} * M_{res(temp)} * M_{res(PPFD)} * M_{res(time)})$$

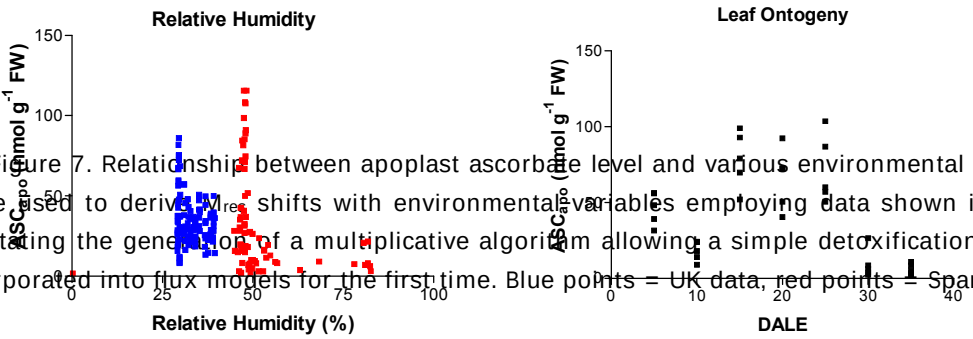


Figure 7. Relationship between apoplast ascorbate level and various environmental variables. Data to be used to derive $V_{max}$ shifts with environmental variables employing data shown in Appendix 1, facilitating the generation of a multiplicative algorithm allowing a simple detoxification module to be incorporated into flux models for the first time. Blue points = UK data, red points = Spanish

(ii) Validation of modelled $M_{res}$ output. There is a need to extend studies examining the importance of ascorbate, and other cell wall-localised compounds, as a first line of defence against ozone-induced oxidative stress through (i) determination of radical scavenging potential of ASC/apoplast fluid (ii) the breaching of apoplast defences in relation to absorbed ozone dose/apoplast scavenging potential and (iii) relationship between genetic variation in flag leaf ASC content and ozone impacts on wheat yield (achievable via measurements on plant material frozen in liquid nitrogen from fumigation experiments conducted during the summer of 2003)

(iii) Review existing data in plant/medical literature. A wider survey of apoplast constitution is required, paying specific attention to potential scavengers of ozone/ROS, rates of reaction, concentrations and turnover in the cell wall. Since there are considerable overlaps between the role of apoplast fluid and respiratory tract lung lining fluid (RTLF) as first lines of defence against external oxidants in plant/humans, respectively, there is a need to draw-down information from the medical literature as well as the plant-based literature.

## Appendix 5.1

Ozone diffusion-reaction network within leaves computed using SODA-model (Plöchl *et al*. 2000, *Planta* **210**: 454-464).

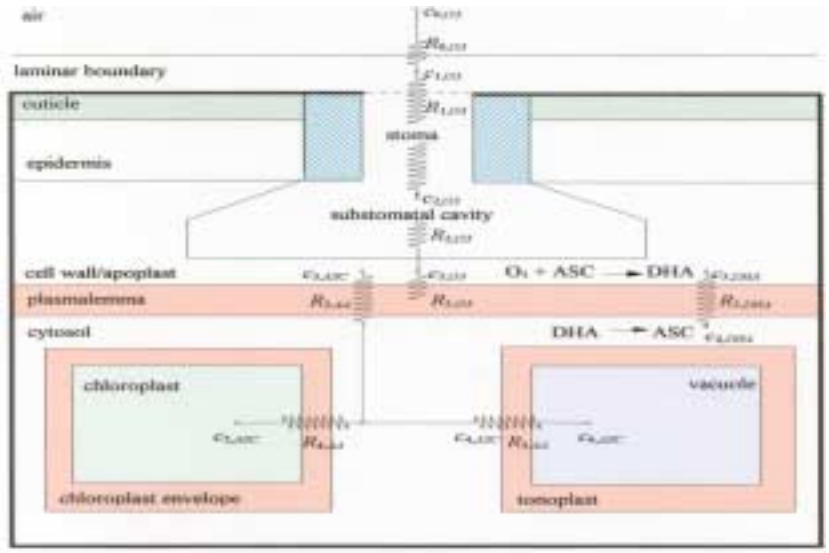


## Appendix 5.2

Ultrastructural parameterization (derived from electron micrographs) and employed $g_s$/ozone concentrations for detoxification modelling performed for field-grown flag leaf of spring wheat. Data for leaves collected at varying times (day/night).

| | **Value** | |
|---|---|---|
| **Input** | **UK** | **Spain** |
| External $O_3$ concentration ($c0.O_3$) | 36 – 39 nmol $mol^{-1}$ | 12 – 45 nmol $mol^{-1}$ |
| Apoplast pH ($pH_3$) | 5.2 – 6.5 | 5.5 – 6.0 |
| Cell wall thickness ($l_3$) | 0.24 – 0.28 µm | 0.396 µm |
| Mesophyll cell surface area ($A_4$) | 2.776 – 3.419 $m^2$ $m^{-2}$ | 2.776 – 3.419 $m^2$ $m^{-2}$ |
| Chloroplast volume ($V_5$) | 0.00384–0.00535 l $m^{-2}$ | 0.00384–0.00535 l $m^{-2}$ |
| Cell wall tortuosity factor (τ) | 0.3 | 0.3 |
| Stomatal conductance ($g_s$) | 50 – 650 mmol $H_2O$ $m^{-2}$ $s^{-1}$ | 35 – 270 mmol $H_2O$ $m^{-2}$ $s^{-1}$ |
| $O_3$-ASC reaction rate constant ($k_{3ASC}$) | 4.8 x $10^7$ $M^{-1}$ $s^{-1}$ | 4.8 x $10^7$ $M^{-1}$ $s^{-1}$ |
| ASC:$O_3$ reaction stoichiometry (σ) | 2:1 | 2:1 |

# 6. Impacts of increasing global background ozone concentrations

Under a contract variation in early 2002, UoB and CEH collaborated in producing an analysis of the impacts of increased global background ozone concentrations on UK ozone exposures and their impacts on vegetation. This was based on an analysis of the implications for the UK of trends, already identified in the NEGTAP (2001) report, of a trend of rising background ozone concentrations, which may offset the decline in maximum concentrations of ozone. The data analysis used the outputs of a global model of background ozone concentrations over the next century (Stevenson et al., 2000), linking this to an analysis of diurnal and seasonal patterns in ozone concentrations at sites in the UK. The results of this analysis for future impacts on vegetation were then assessed.

This analysis drew some important conclusions of direct relevance to the overall objectives of this contract. In particular, new assessments based on ozone flux models demonstrate that significant ozone fluxes may occur in sensitive species at external ozone concentrations in the range 20-40 ppb. The major impact of changes in global background concentrations in the next 2-3 decades will be on concentrations in this range. This demonstrates that the flux-based approach is better suited to assessing future changes in ozone climate than is the AOT40 approach.

The full report of this part of the work programme was submitted to DEFRA in March 2002; the Executive Summary is included as Annex 4 of this Report. The full report is available on the CEH website (http://www.nbu.ac.uk/pollution/docs/O3trends_Ukveg.htm). The significance of this analysis was indicated by a request from the leading atmospheric science journal Atmospheric Environment for an overview of the project to be submitted as a 'New Directions' articles, which identifies new issues and information of wide policy significance. This was published as Coyle et al. (2003).

# 7 Contributions to Policy Development

This section briefly describes how the work under this project has contributed to the development and acceptance of flux-based risk assessment methods for ozone within UN/ECE. It firstly describes the contribution to two meetings in 2002 that considered the current status of deposition models and the development of new critical levels. It then summarises the contribution to the development of the new deposition module within the new Unified EMEP model. Finally, it considers the contribution to sections of the new chapter of the Mapping Manual (under the ICP Mapping and Modelling) that describe new methods for mapping flux-based critical levels.

## 7.1. Organisation and Participation in UN/ECE Workshops

The new methods for modelling ozone deposition and flux were discussed in two meetings within UN/ECE that were held in 2002. These meetings were extremely important in allowing the new methods to be subjected to rigorous review by international experts within the context of the policy applications envisaged within UN/ECE. The first of these, an Expert Panel meeting to discuss ozone deposition, held under the joint auspices of EMEP and ICP Vegetation, was organised as part of the work programme of this contract. The Expert Panel meeting was held in Harrogate in June 2002. The event was very successful, attracting 37 experts from 12 different countries, including representatives from the Working Group on Effects, the Coordination Centre for Effects, ICP Vegetation and EMEP. The participants include a balanced mix of experts on deposition, on stomatal modelling and on ozone flux-effect modelling. Consistent conclusions were reached from each of the three working groups, enabling the meeting to agree clear and strong recommendations. The Summary Report of the meeting, which is attached as Annexe 5 of this Report, was presented in August 2002 to the annual Task Force meeting in Geneva. The three key conclusions reached were:-

a) that the AOT40 index provides an incorrect assessment of the regional distribution of the risk of damage to vegetation across Europe.

b) that flux-based risk assessment methods offer the potential for improved evaluation and should be recommended for future application within the Convention.

c) that the deposition and flux algorithm now implemented within the EMEP model provides an adequate basis for first estimation and application of flux-based critical levels.

The funding to support this workshop which was provided by Defra was used strategically in two ways:- (i) to encourage the attendance of leading European experts on deposition and flux; and (ii) to facilitate the attendance of a group of leading US experts in modelling flux and deposition. The active involvement of US experts proved to be valuable in providing further independent critical review of the flux and deposition models developed under this contract and ensured that discussion at the Workshop took full account of the latest US developments. It was also beneficial that Dr. Emberson

was able to attend the US National Air Pollution Workshop in April 2002, to ensure that the US experts were well-briefed on current European ideas and hence to gain the maximum benefit from this interaction. The participation of US experts also led to concrete plans for collaboration, for example by providing access on flux and deposition data for crops in regions of the US with a Mediterranean climate, hence providing the new opportunities to test the model which were described in Section 2 of this Report.

The results of the Harrogate workshop provided a basis from which analysis of flux-response relationships and estimation of critical fluxes proceeded for evaluation at the second workshop, which was held in Gothenburg in November 2002. This workshop discussed revisions of critical levels of ozone, including the development of new flux-based critical levels. Close communication was maintained with the organisers of the Gothenburg workshop, to ensure that the results of the Harrogate meeting were well-matched to the planned structure of the Gothenburg meeting, partly though membership of the Scientific Steering Committee for this meeting. Prof. Ashmore spoke at an early stage of the Gothenburg workshop, to ensure that all participants were well appraised of the results of the Harrogate meeting, and to provide an overview of the current status of flux modelling. The outcomes of this workshop are considered further in Section 7.3 below.

We have been successful in negotiating a special issue of the journal Atmospheric Environment devoted to the results of key papers presented at the Harrogate and Gothenborg workshops. This special issue will be edited by Dr. Emberson and Prof. Ashmore, in collaboration with Dr. Karlsson and Dr. Pleijel, organisers of the Gothenburg workshop. The publication of this special issue in early 2004 will be an important mechanism for dissemination of the results of this project, and related work on flux and deposition modelling. Section 8 (Dissemination) summarises the verbal and poster presentations made on work related to this project at the two workshops, as well as at annual meetings of ICP Vegetation and at the US Air Pollution Workshop.

## 7.2 Development of integrated EMEP deposition model

The integration of the deposition module with the EMEP photochemical model has been an iterative process involving discussions between SEI & UoB and Dr. David Simpson of EMEP. These discussions have resulted in i) the implementation of the SEI land cover database for both deposition and stomatal flux estimates; ii) the identification of further data needs related to land cover and establishment of methods to supply these data (e.g. variations in LAI across Europe; improved irrigation and agricultural data) and iii) ensuring that the EMEP model is coded correctly and that any necessary modifications to the existing model formulation and structure are performed.

The work on the land-cover database was described in Section 4 of this Report. Evaluation of the deposition model performed by Tuovinen et al. (1999) highlighted the importance of the Leaf Area Index (LAI) parameter in obtaining model estimates close to observed values, and this has been identified as the key priority in terms of developing the database. Currently, the deposition model uses default LAI values for specific deposition land-cover classes. This allows variation between cover-classes but not within these classes across Europe. It is acknowledged that LAI will vary with climate (being particularly sensitive to extremes of temperature and soil moisture) and also, for certain cover-classes such as forests, with local management (sylvicultural) practices. Work is in progress to identify pan European datasets that may be useful in determining the variation in LAI across Europe. For example, the FIRS database provides information that stratifies European forests into "homogenous" forest eco-types. These data have been obtained from FIRS (now re-named as the Eurolandscape project) and work is in progress to identify ways in which certain data parameters (e.g. stand height, stand density and stand management data) may be helpful in describing the variation in LAI across Europe for forest tree species. This land-cover type is seen as the priority for this research since LAI values are likely to show the greatest variation relative to the other cover-types. The final task has been accomplished by collaboration with work conducted at CEH Edinburgh, to develop and code a stand-alone "box model" of the deposition model with a view to enabling dry deposition of a number of different gaseous pollutants (i.e. not solely $O_3$). The new FORTRAN code for the revised deposition module, within the new Unified EMEP Model, was developed by Margaret McDougall and Ron Smith at CEH Edinburgh, in close collaboration with David Simpson at EMEP, using the formulations and parameterisations developed for ozone within this project.

The current status of the EMEP deposition model is now documented as part of the description of new Unified EMEP model in EMEP Status Report 1/2003 (Simpson et al, 2003a). Annexe 6 of this Report summarises the modelling of both AOT40 and flux in this new model. Simpson et al. (2003b) provide a comparison of the modelled ozone concentrations with the new Unified EMEP model, using the revised deposition module, with measured data across Europe. The key section of this longer report is provided as Annexe 7 of this Report. The results have shown that the best model performance is for daily ozone maximum ozone concentrations, for which daily correlation coefficients are generally above 0.8 across Europe. For most years the modelled and observed frequency distributions agree rather well with the average bias for daily ozone maximum

concentrations being below 12%. The worse performance of the EMEP model was in the eastern Mediterranean regions and probably related to the choice of boundary conditions. It is, however, important to note that the performance of the model reflects many substantive changes to the whole photochemical model, and not simply the effect of the new deposition module to which this project has contributed.

The integration of the deposition module with the EMEP photochemical model has enabled, for the first time, preliminary modelling and mapping of ozone flux to be performed across Europe. A report of the modelled fluxes, including a comparison with modelled AOT40, is given in Annex 8 of this Report (Simpson et al., 2002). This report is also available from http://www.emep.int/. In summary, this report describes preliminary modelling and mapping of ozone deposition, performed for the year 1999, that is capable of differentiating between stomatal and non-stomatal ozone flux, and as such enables estimates of absorbed ozone dose to be made for different vegetation types as a component of total deposition. It is emphasised that the results from these initial model predictions are presented for illustration only. Work is still required to improve many of the input databases (e.g. the description of LAI across Europe and phenological predictions) to the new model and to deal with soil moisture effects, before proper estimates of ozone uptake can be made. However, the basic features of the ozone uptake modelling presented here are believed to represent a reasonable first estimate of the spatial and temporal patterns of ozone uptake that exist across Europe.

The results, which are shown in Annexe 8, allow a number of important conclusions to be made. Firstly, it seems clear that spatial patterns of AOT40 across Europe are very different from those of stomatal uptake and deposition. Ozone uptake rates have a much more uniform distribution across Europe than AOT40. The difference between AOT40 and uptake is largely due to the fact that in central and southern Europe, the meteorological conditions which favour ozone formation (high temperatures, and hence high vapour pressure deficits) tend to reduce stomatal conductance and hence ozone uptake. Thus, elevated ozone can contribute to the AOT40 index but not to uptake. In contrast, in northern Europe the cooler more humid conditions tend to increase stomatal conductance under typical conditions causing even moderate ozone concentrations to result in significant levels of ozone uptake to the plant. As such, concentrations of ozone below 40 ppb (common in northern areas), which are discounted entirely in the AOT40 index, may contribute to ozone uptake rates.

## 7.3. Development and Application of Flux-based Critical Levels

The flux models, and their application in deriving flux-response relationships for wheat, potato and young trees, which were developed in collaboration with colleagues in Sweden, were critically evaluated at the Gothenburg workshop. The conclusions about flux-response relationships and their use in deriving flux-based critical levels, differed between the three working groups as follows:-

a) for semi-natural vegetation, it was concluded that flux-based approaches had not been developed to the stage at which they could be applied

b) for forest trees, flux-based critical levels were recognised as one of three potential approaches

c) for agricultural crops, the use of flux-based critical levels based on flux-response relationships for wheat and potato was accepted . A flux-based short-term critical level for use with clover was also adopted.

The detailed conclusions of the Gothenburg workshop can be found at http://www.ozoneworkshop.ivl.se.

For all cases in which the use of critical fluxes was accepted in principle at the Gothenburg workshop, it was not possible to provide detailed information on the precise formulation and parameterisation of the flux models to be used. These were developed after the meeting through collaboration between several research groups, including those involved in this project. A further meeting was therefore held at Manchester in April 2003, to move from the general recommendations made at the Gothenburg workshop to agree the final version of the derivation of flux-response models and of methods to map ozone fluxes for comparison with the new flux-based critical levels. Because of the policy significance of detailing these models, and providing inputs to the new Critical Levels chapter of the Mapping Manual, significant staff time was, in consultation with the Defra project officer, devoted to this task rather than to some of the planned activities in the final year of this project.

The outcome of this work was that the draft Chapter of the Mapping Manual which was produced at the Manchester meeting was formally adopted by ICP Mapping and Modelling for use in national and international mapping of ozone flux, and exceedance of flux-based critical levels. A full description of the flux methods developed can be found in the UN/ECE "Manual on Methodologies and Criteria for Mapping Critical Levels/Loads and geographical areas where they are exceeded" (http://www.oekodata.com/icpmapping/html/manual.html.). Annexe 9 of this report provides a copy of those sections of the new Mapping Manual to which the work under this contract has contributed.

The methods which have now been formally adopted still need to be applied by individual countries, and is likely that some further modification of the models will be made as more experience is gained by a wider range of scientific groups and mapping experts in different countries across Europe. We are already working actively with national groups in Sweden and Belgium, in terms of applying the Mapping Method methods to national datasets

In summary, the work under this project has made a very significant contribution to the development of new methods of modelling deposition and stomatal flux of ozone, which have now been accepted for application with the UN/ECE, and are likely to be used in evaluation of emission control scenarios in the revision of the Gothenburg Protocol which is planned for 2005-6.

.

# 8 Dissemination

## (a) Published peer-reviewed papers and book chapters


Barnes JD**,** Zheng Y, Lyons TM (2002) Plant resistance to ozone: the role of ascorbate. In*: Air Pollution and Plant Biotechnology* (ed. by K. Omasa, H.Saji, S. Youssefian & N. Kondo). Springer-Verlag, Tokyo. pp 235-252

Coyle M, Fowler D & Ashmore MR (2003). Implications of increasing tropospheric ozone concentrations for vegetation. *Atmospheric Environment*, 37, 153-154.

Emberson, L.D. Simpson, D., Tuovinen, J.-P., Ashmore, M.R., and Cambridge, H.M. (2001) Modelling and mapping ozone deposition in Europe. *Water, Air and Soil Pollution* **130**: 577-582

Maddison J, Lyons TM, Plöchl M, Barnes JD (2002) Hydroponically-cultivated radish fed L-galactono-1,4-lactone exhibit increased tolerance to ozone. *Planta* **214**: 383-391

Pignocchi C, Fletcher JM, Barnes JD, Foyer CH (2003) The function of ascorbate oxidase (AO) *in planta. Plant Physiology* **132**: 1631-1641.

Sanmartin M, Drogoudi PD, Lyons TM, Petraki I, Barnes J, Kanellis A (2003) Over-expression of ascorbate oxidase in the apoplast of transgenic tobacco results in altered ascorbate and glutathione redox states and increased sensitivity to ozone. *Planta* 216: 918-928

Simpson, D., Tuovinen, J.-P., Emberson, L. and Ashmore, M. (2001) Characteristics of an ozone deposition module. *Water, Air and Soil Pollution*: Focus **1**, 253-262.

Simpson, D., Tuovinen, J.-P., Emberson, L.D. and Ashmore, M.R. (2003) Characteristics of an ozone deposition module II: Sensitivity analysis. *Water, Air and Soil Pollution* 143: 123-137

Tuovinen, J.-P., Simpson, D., Mikkelsen, T. N., Emberson, L. D., Ashmore, M. R., Aurela, M., Cambridge, H. M., Hovmand, M. F., Jensen, N. O., Laurila, T., Pilegaard, K. and Ro-Poulsen, H. (2001) Comparisons of measured and modelled ozone deposition to forests in Northern Europe. *Water, Air and Soil Pollution*: Focus **1**, 263-274.

Tuovinen, J.-P., Emberson, L.D., Simpson, D., Ashmore, M.R., Aurela, M. and Cambridge, H.M. (2001) A new dry deposition module for ozone: comparisons with measurements. In: P. Midgley, M. Reuther & M. Williams (Eds.), Proceedings from the EUROTRAC-2 Symposium 2000, Springer-Verlag, Berlin, Germany.

(b) Peer-reviewed papers submitted in 2002-3:-

Coyle, M., Emberson, L.D., Levy, P., Murray, M., Nemitz, E., Ashmore, M.R. and Fowler, D. Assessment of the EMEP ozone deposition model: Comparison with Measurements of stomatal conductance for grassland (Easter Bush, Scotland) at leaf and canopy scales. (Submitted to *Atmospheric Environment*).

Karlsson, P.E., Uddling, J., Braun, S., Broadmeadow, M., Elvira, S., Gimeno, B.S., Le Thiec, D., Oksanen, E., Vandermeiren, K., Wilkinson, M., Emberson, L. D. New Critical Levels for Ozone Impact on Trees Based on AOT40 and Leaf Cumulated Uptake of Ozone. (Submitted to *Atmospheric Environment*).

Pignocchi C, Fletcher JM, Wilkinson JE, Barnes JD, Foyer CH (2003) Redox control of signalling in the apoplast is modulated by ascorbate oxidase. *The Plant Journal*, resubmitted August 2003.

Tuovinen, J.-P, Ashmore, M.R., Emberson, L.D., Simpson, D. Testing and improving the EMEP ozone deposition module. (Submitted to *Atmospheric Environment*).

Wieser, G. and Emberson, L.D. Evaluation of the stomatal conductance formulation in the EMEP ozone deposition model for Picea abies. (in press in Atmospheric Environment)

(c) Other Reports on, or Associated with the Project

Ashmore MR, Coyle M & Fowler D (2002). Implications of increasing tropospheric background ozone concentrations for vegetation in the UK. Report to DEFRA available at: http://www.Edinburgh.ceh.ac.uk/pollution/

Cinderby, S. (2002) Description of 2002 revised SEI land cover map. http://www.york.ac.uk/inst/sei/APS/projects.html

EMEP Report 1&2/01, July 2002. Transboundary acidification and eutrophication and ground level ozone in Europe. EMEP Status Report 2002. Joint CCC & MSC-W Report. http://www.emep.int/reports/emep_report_1_2_2002.pdf

Simpson D, Ashmore M, Emberson L, Tuovinen J-P, Macdougall M & Smith RI (2002). Stomatal ozone uptake over Europe: preliminary results. In: Transboundary Acidification, Eutrophication and Ground Level Ozone in Europe. EMEP Report 1&2, 2002. Norwegian Meteorological Institute, Oslo.

### (d) Contributions to the Harrogate Expert Panel meeting

Written papers included in the Background Documents for the meeting:

- Introduction and aims of the meeting (Ashmore)
- Data requirements for ozone flux modelling on a regional scale (Emberson)
- Description of 2002 revised SEI land-cover map (Cinderby et al.)
- Stomatal conductance: key factors in controlling ozone flux into the leaves of forest trees (Wieser & Emberson)
- Modelling stomatal conductance and ozone flux for NC-S and NC-R white clover (*Trifolium repens*) biotypes: statistical and multiplicative flux modelling (Mills, Hayes & Emberson)

Oral presentations:

- Overview of workshop aims and planning (Ashmore)
- EMEP model and its link to policy evaluation (Simpson)
- Modelling stomatal flux (Emberson)
- Evaluating the performance of deposition models (Tuovinen)
- Long-term ozone flux measurements and the role of non-stomatal deposition (Fowler)
- Intrinsic factors governing the critical flux of ozone at a leaf level (Barnes)
- Description of SEI land-cover map (Cinderby)
- Comparison of the EMEP box model with ozone flux measurements over grasslands, wheat and sugar beet (Coyle)

### (e) Contributions to the Gothenburg workshop

Contributions to Workshop Proceedings:

- Report from the working group on agricultural crops (Mills & Emberson)
- Report from the working group on semi-natural vegetation (Ashmore, Franzaring)
- How well can we model ozone fluxes (Ashmore)
- Stomatal ozone uptake over Europe: preliminary results (Simpson, Ashmore, Emberson, Tuovinen, Macdougall, Smith)

- Introducing response modifying factors into a risk assessment for ozone effects on crops in Europe (Mills, Holland, Buse, Cinderby, Hayes, Emberson, Cambridge, Ashmore, Terry)
- Developing ozone-flux effect models for white clover from the ICP Vegetation ambient air monitoring experiment (Mills, Bueker, Hayes, Emberson, Werner, Gimeno, Fumigalli, Kollner, Manes, Pihl-Karlsson, Soja, Vandermeiren)
- Ozone critical levels for semi-natural vegetation (Fuhrer, Ashmore, Mills, Hayes, Davison)
- New critical levels for ozone impact on trees based on AOT40 and leaf cumulated ozone uptake (Karlsson, Uddling, Braun, Broadmeadow, Elvira, Gimeno, Le Thiec, Oksanen, Vandermeiren, Wilkinson, Emberson)
- Stomatal conductance: key factors controlling ozone flux into the leaves of forest trees: a case study in *Picea abies* (Wieser, Emberson)

## (f) Other oral and poster presentations

Oral presentations:

- UNECE/EMEP Flux Modelling/Mapping Workshop, Manchester
- APPM Symposium, Poland
- Annual ICP Vegetation meeting 2001, 2002 and 2003
- US Air Pollution Workshop 2001 and 2003
- UK Air Pollution Workshops (CAPER) 2001, 2002 and 2003
- Japanese Air Pollution Workshop 2001

Poster presentations:

- Annual ICP Vegetation meeting, 2001, 2002 and 2003
- UK Air Pollution Workshops 2001, 2002 and 2003.
- US Air Pollution Workshops 2001,2002 and 2003
- Japanese Air Pollution Workshop 2001
- European Science Foundation Workshop 2001 ‘Adaptation of Plant Populations to Environmental Insult’

# 9 References


Altimir, N., Tuonvinen, J.-P., Vesala, T., Kulmala, M & Hari, P. (in press). Measurements of ozone removal to Scots pine shoots: calibration of a stomatal uptake model including the non-stomatal component. *Atmospheric Environment*.

Aranda, A., Gil, L., Pardos, J.A. (2002) Physiological responses of *Fagus sylvatica* L. seedlings under *Pinus sylvestris* L. and *Quercus pyrenaica* Willd. overstories. *Forest Ecology and Management*, **162**: 153-164

Araus JL, Alerge L, Tapia L & Calafell R (1986), Relationship between leaf structure and gas exchange in wheat leaves at different insertion levels. *Journal of Experimental Botany*, **37**, 1323-1333.

Bassin S., Calance P., Weidinger T., Gerosa G., Fuhrer J. (in press) Modelling of seasonal ozone fluxes to grassland and wheat with ODEM: model improvement, testing and application. *Atmospheric Environment*.

Baumgarten, M., Werner, H., Haberle, K.-H., Emberson, L.D., Fabian, P. & Matyssek, R. (2000). Seasonal ozone response of mature beech trees (*Fagus sylvatica*) at high altitude in the Bavarian forest (Germany) in comparison with young beech grown in the field and in phytotrons. *Environmental Pollution*, **109:** 431-442.

Beadle, C.L., Talnot, H., Jarvis, P.G. (1982) Canopy structure and leaf area index in a mature Scots pine forest. *Forestry* **55**: 105-123

Caldwell, M.M., Meister, H.-P., Tenhunen, J.D. & Lange, O.L. (1986. Canopy structure, light microclimate and leaf gas exchange of *Quercus coccifera* L. in a Portuguese macchia: measurements in different canopy layers and simulations with a canopy model. *Trees*, **1**: 25-41.

Cinderby, S. (2002) Description of 2002 revised SEI land cover map. http://www.york.ac.uk/inst/sei/APS/projects.html

Coyle M, Fowler D & Ashmore MR (2003). Implications of increasing tropospheric ozone concentrations for vegetation. *Atmospheric Environment*, **37**: 153-154.

Coyle, M., Emberson, L.D., Levy, P., Murray, M., Nemitz, E., Ashmore, M.R. and Fowler, D. Assessment of the EMEP Ozone Deposition Model: Comparison with measurements of stomatal conductance for grassland (Easter Bush, Scotland) at leaf and canopy scales. Submitted to *Atmospheric Environment*.

de Smet, P.A.M. and Hettelingh, J.-P. (2001) Intercomparison of current European land use/land cover databases. CCE status report 2001.

Defra Statistics. http://statistics.defra.gov.uk/esg/publications/auk/

Elvira, S., Bermejo, V, Manrique, E., Gimeno, B.S. (in press). On the response of two populations of *Quercus coccifera* to ozone and its relationship with ozone uptake. *Atmospheric Environment*.

Emberson, L.D. (1997) Defining and mapping relative potential sensitivity of European vegetation to ozone. PhD Thesis. Imperial College, University of London.

Emberson, L.D., Simpson, D., Tuovinen, J.-P., Ashmore, M.R., Cambridge, H.M., (2000a). *Towards a model of ozone deposition and stomatal uptake over Europe*. EMEP/MSC-W Note 6/2000. Norwegian Meteorological Institute, Oslo, 58 pp.

Emberson, L.D., Wieser, G. and Ashmore, M.R. (2000b). Modelling of stomatal conductance and ozone flux of Norway spruce: comparisons with field data. *Environmental Pollution*, **109**: 393-402.

Falge, E., Graber, W., Siegwolf, R. and Tenhunen, J.D. (1996) A model of the gas exchange response of *Picea abies* to habitat conditions. *Trees* **10**: 277-287

Gerosa, G., Cieslik, S., Ballarin-Denti, A. (2003). Ozone dose to a wheat field determined by the micrometeorological approach. *Atmospheric Environment*, **37** : 777-788.

Heath, J. (1998). Stomata of trees growing in $CO_2$ enriched air show reduced sensitivity to vapour pressure deficit and drought. *Plant, Cell and Environment*, **21**: 1077-1088

Karlsson, P.-E., Sellden, G. & Pleijel, H. (eds.) (2003). Establishing Ozone Critical Levels II. UN/ECE Workshop Report. Report B1523, IVL Publications, Stockholm. Available at http://www.ozoneworkshop.ivl.se

Karlsson, P.E., Uddling, J., Braun, S., Broadmeadow, M., Elvira, S., Gimeno, B.S., Le Thiec, D., Oksanen, E., Vandermeiren, K., Wilkinson, M. & Emberson, L. D. (in press). New critical levels for ozone impact on trees based on AOT40 and leaf cumulated uptake of ozone. *Atmospheric Environment*.

Lange, O.L., Heber, U., Schulze, E.D., Ziegler, H., (1989) Atmospheric pollutants and plant metabolism. In: Schulze ED, Lange OL, Oren R (eds) *Forest decline and air pollution: a study of spruce (Picea abies) on acid soils*. Ecological studies, Vol. 77, Springer, Berlin Heidelberg New York, pp. 238-273

Maddison J, Lyons TM, Plöchl M, Barnes JD (2002) Hydroponically-cultivated radish fed L-galactono-1,4-lactone exhibit increased tolerance to ozone. *Planta* **214**: 383-391

Massman, W.J. and Grantz, D.A. (1995) Estimating canopy conductance to ozone uptake from observations of evapotranspiration at the canopy scale and at the leaf scale. *Global Change Biology* **1**: 183-198

Massman, W.J., Pederson, J., Delany, A., Grantz, D., den Hartog, G., Oncley, S.P., Pearson, Jr. R, Shaw, R. (1994) An evaluation of the RADM surface module for ozone uptake at three sites in the San Joaquin Valley of California. *Journal of Geophysical Research* **99**: 8281-8294

Nali, C., Paoletti, E., Marabottini, R., Della Rocca., G., Lorenzini, G., Paolacci, A.R., Ciaffi, M., Badiani, M. (in press). Ecophysiological and biochemical strategies of response to ozone in Mediterranean evergreen species. *Atmospheric Environment*.

NEGTAP (2001). *Trans-boundary Air Pollution: Acidification, Eutrophication and Ground-level Ozone in the UK.* Report of the National Expert Group on Trans-boundary Air Pollution. Department of Environment, Food and Rural Affairs, London.

Norman, J.M. (1982). Simulation of microclimates. In: Hatfield, J.L. and Thompson, I.J. (eds.). *Biometeorology in Integrated Pest Management*. Academic Press, New York, pp. 65-99.

Pedersen, J.R., Massman, W.J., Mahrt, L., Delany, A., Oncley, S., den Hartog, G., Neumann, H.H., Mickle, R.E., Shaw, R.H., Paw, K.T., Grantz, D.A., Macpherson, J.I., Desjardins, R., Scheupp, P.H., Pearson Jr., R. and Arcado, T.E. (1995) Californian ozone deposition experiment: methods, results, and opportunities. Atmos. Environ. 29: 3115-3132

Pignocchi C, Fletcher JM, Barnes JD, Foyer CH (2003a) The function of ascorbate oxidase (AO) *in planta. Plant Physiology* **132**: 1631-1641.

Pignocchi C, Fletcher JM, Wilkinson JE, Barnes JD, Foyer CH (2003b) Redox control of signalling in the apoplast is modulated by ascorbate oxidase. *The Plant Journal*, resubmitted August 2003

Plochl, M., Lyons, T.M., Ollernshaw, J.H. & Barnes, J.B. (2000). Simulating ozone detoxification in the leaf apoplast through direct reactions with ascorbate. *Planta*, 210, 454-469.

Raftoyannis, Y. and Radoglou, K. (2002) Physiological responses of beech and sessile oak in a natural mixed stand during a dry summer. *Annals of Botany* **89**: 723-730

Sanmartin M, Drogoudi PD, Lyons TM, Petraki I, Barnes J, Kanellis A (2003) Over-expression of ascorbate oxidase in the apoplast of transgenic tobacco results in altered ascorbate and glutathione redox states and increased sensitivity to ozone. *Planta* **216**: 918-928

Simpson, D., Ashmore, M.R., Emberson, L.D., Tuovinen, J.-P., Macdougall, M. & Smith, R.I. (2002). Stomatal uptake over Europe: preliminary results. In*: Transboundary Acidification, Eutrophication and Ground-Level Ozone over Europe.* EMEP Report 1&2/2002, pp. 63-71. .Norwegian Meteorological Institute, Oslo.

Simpson, D., Fagerli, H., Jonson, J.E., Tsyro, S., Wind, P. & Tuovinen, J-P (2003a). *Transboundary Acidification, Eutrophication, and Ground-Level Ozone in Europe*. EMEP Status Report 1. Part I: Unified EMEP model description. Norwegian Meteorological Institute, Oslo.

Simpson, S., Tuovinen, J.-P., Emberson, L.D. & Ashmore, M.R. (2003b). Characteristics of an ozone deposition module II: sensitivity analysis. *Water Air and Soil Pollution*, 143, 123-137.

Stevenson, D.S., Johnson, C.E. et al. (2000). Future estimates of tropospheric ozone radiative forcing and methane turnover. *Geophysical Research Letters* 27: 2073-2076.

Sturm, N., Kostner, B., Hartung, W. and Tenhunen, J.D. (1998) Environmental and endogenous controls on leaf- and stand-level water conductance in a Scots pine plantation. *Annales des Sciences Forestieres* 55: 237-253

Tognetti, R., Longobucco, A., Miglietta, F., and Raschi, A. (1998) Transpiration and stomatal behaviour of *Quercus ilex* plants during the summer in a Mediterranean carbon dioxide spring. *Plant, Cell and Environment* 21: 613-622

Tuovinen J.-P., Aurela, M. & Laurila, T. (1999). Measured and modelled ozone deposition to three different ecosystems in Finland. In: P.M. Borrell and P. Borrell (eds.) Proceedings of the EUROTRAC Symposium '98, WIT Press, Southampton, pp. 197-201

Tuovinen, J.-P., Ashmore, M.R., Emberson, L.D., Simpson, D. (in press). Testing and improving the EMEP ozone deposition model. *Atmospheric Environment*

Tuovinen, J.-P., Emberson, L.D., Simpson, D., Ashmore, M.R., Aurela, M. and Cambridge, H.M., (2001a). A new dry deposition module for ozone: comparisons with measurements. In: P. Midgley, M. Reuther & M. Williams (Eds.), Proceedings from the EUROTRAC-2 Symposium 2000, Springer-Verlag, Berlin, Germany.

Tuovinen, J.-P., Simpson, D., Mikkelsen, T. N., Emberson, L. D., Ashmore, M. R., Aurela, M., Cambridge, H. M., Hovmand, M. F., Jensen, N. O., Laurila, T., Pilegaard, K. and Ro-Poulsen, H. (2001b) Comparisons of measured and modelled ozone deposition to forests in Northern Europe. *Water, Air and Soil Pollution*: Focus 1, 263-274.

UN/ECE Manual on Methodologies and Criteria for Mapping Critical Levels/Loads and geographical areas where they are exceeded. (2003). http://www.oekodata.com/icpmapping/html/manual.html

Wang, K.-Y. (1996) Canopy $CO_2$ exchange of Scots pine and its seasonal variation after four-year exposure to elevated $CO_2$ and temperature. *Agricultural Forest Meteorology* 82: 1-27

Wieser, G. & Emberson, L.D. (in press). Stomatal conductance: key factors in controlling ozone flux into the leaves of forest trees: a case study in *Picea abies*. *Atmospheric Environment*.

Zhang, L., Moran, M.D. & Brook, J.R. (2001). A comparison of models to estimate in-canopy photosynthetically active radiation and their influence on canopy stomatal resistance. *Atmospheric Environment*, 35, 4463-4470.